

Biogeosciences Discussions is the access reviewed discussion forum of *Biogeosciences*

**Anthropogenic CO₂
in the Atlantic Ocean**

M. Vázquez-Rodríguez
et al.

An upgraded carbon-based method to estimate the anthropogenic fraction of dissolved CO₂ in the Atlantic Ocean

M. Vázquez-Rodríguez¹, X. A. Padin¹, A. F. Ríos¹, R. G. J. Bellerby^{2,3}, and F. F. Pérez¹

¹Instituto de Investigaciones Marinas, CSIC, Eduardo Cabello 6, 36208 Vigo, Spain

²Bjerknes Centre for Climate Research, University of Bergen, Allégaten 55, 5007 Bergen, Norway

³Geophysical Institute, University of Bergen, Allégaten 70, 5007 Bergen, Norway

Received: 24 March 2009 – Accepted: 18 April 2009 – Published: 29 April 2009

Correspondence to: M. Vázquez-Rodríguez (mvazquez@iim.csic.es)

Published by Copernicus Publications on behalf of the European Geosciences Union.

Title Page

Abstract

Introduction

Conclusions

References

Tables

Figures

◀

▶

◀

▶

Back

Close

Full Screen / Esc

Printer-friendly Version

Interactive Discussion

Abstract

An upgrade of classical methods to calculate the anthropogenic carbon (C_{ant}) signal based on estimates of the preformed dissolved inorganic carbon (C_{T}°) is proposed and applied to modern Atlantic sections. The main progress has been the use of sub-surface layer data (100–200 m) to reconstruct water mass formation conditions and obtain better estimates of preformed properties. This practice also eliminates the need for arbitrary zero- C_{ant} references that are usually based on properties independent of the carbon system, like the CFC content. The long-term variability of preformed total alkalinity (A_{T}°) has been considered and the temporal variability of the air-sea CO_2 disequilibrium (ΔC_{dis}) included in the formulation. The change of ΔC_{dis} with time has shown to have non-negligible biases on C_{ant} estimates, producing a $4 \mu\text{mol kg}^{-1}$ average decrease. The proposed $\varphi C_{\text{T}}^{\circ}$ method produces substantial differences in the C_{ant} inventories of the Southern Ocean and Nordic Seas ($\sim 18\%$ of the total inventory for the Atlantic) compared with recent C_{ant} inventories. The overall calculated Atlantic C_{ant} inventory referenced to 1994 is $55 \pm 13 \text{ Pg C}$, which reconciles the estimates obtained from classical C_{T}° -based C_{ant} calculation methods, like the ΔC^* , and newly introduced approaches like the TrOCA or the TTD methods.

1 Introduction

The world oceans sequester annually $2.2 \pm 0.4 \text{ Pg C}$ out of the total $7.4 \pm 0.5 \text{ Pg yr}^{-1}$ of anthropogenic carbon (hereinafter denoted by C_{ant}) emitted to the atmosphere from activities such as fossil fuel burning, land use changes, deforestation and cement production (Siegenthaler and Sarmiento, 1993; Sabine et al., 2004; IPCC, 2007). The Atlantic Ocean alone contributes with a share of 38% to the anthropogenic oceanic carbon storage (Sabine et al., 2004) notwithstanding its moderate surface area (29% of the global ocean).

Since C_{ant} cannot be measured directly it has to be deduced from the Total Inor-

BGD

6, 4527–4571, 2009

Anthropogenic CO_2 in the Atlantic Ocean

M. Vázquez-Rodríguez
et al.

Title Page

Abstract

Introduction

Conclusions

References

Tables

Figures

◀

▶

◀

▶

Back

Close

Full Screen / Esc

Printer-friendly Version

Interactive Discussion



ganic Carbon (C_T) pool, out of which the anthropogenic signal represents a relatively small fraction ($\sim 3\%$). To tackle the intricate and full of uncertainties issue of knowing how much C_{ant} there is and where in the ocean is stored the carbon-based “back-calculation” techniques were pioneered (Brewer, 1978; Chen and Millero, 1979). The philosophy behind these methods goes through realizing that the preformed C_T (C_T° , the existing C_T when a water mass is formed) has not remained constant ever since the beginning of the industrial revolution. Surface waters gradually started sensing the effect of rising partial pressures of atmospheric CO_2 ($p\text{CO}_2^{\text{atm}}$), which forced more of this gas to dissolve (Brewer, 1978). From this perspective, it was argued that the C_{ant} imprint concealed in C_T° could be reckoned by deducting from it a preindustrial “zero- C_{ant} ” reference, namely $C_{\text{ant}} = C_T^\circ - C_T^{\circ\pi}$ (the superscript “ π ” will denote “at the preindustrial era” hereinafter).

Over the years a series of improvements and contributions have been added to this initial “preformed carbon” C_{ant} estimation approach (Wallace, 2001). These went from more realistic assumptions on water mass equilibration and formation conditions to better estimates of $C_T^{\circ\pi}$ and MLR fits from surface or near-surface observations to calculate preformed total alkalinity (A_T°) (Gruber et al., 1996; Körtzinger et al., 1998; Pérez et al., 2002; Ríos et al., 2003; Lo Monaco et al., 2005). There exist some approaches that cannot be denoted as C_T° -based methods yet they have added to our knowledge of C_{ant} estimation by introducing new constraints. For instance, the transient time distribution (TTD) (Vaugh et al., 2006) is an indirect method fully detached from the need of carbon system measurements that assumes there is a distribution of ventilation times (i.e., the TTD) and uses age estimates from CFCs to determine the moment when water masses were last in contact with the atmosphere.

One of the most crucial aspects in any C_T° -based approach in order to obtain accurate C_{ant} estimates is reconstructing water mass formation (WMF) conditions as faithfully as possible. This is most relevant for calculating preformed nutrient concentrations and, primarily, A_T° and the extent of air-sea CO_2 and O_2 equilibria. The original back-calculation methods assumed full-saturation of water masses in terms of oxygen, CO_2

**Anthropogenic CO_2
in the Atlantic Ocean**M. Vázquez-Rodríguez
et al.

Title Page

Abstract

Introduction

Conclusions

References

Tables

Figures

◀

▶

◀

▶

Back

Close

Full Screen / Esc

Printer-friendly Version

Interactive Discussion



and CFCs at the time of outcropping. The CO₂ air-sea disequilibrium term (ΔC_{dis}) first formal estimation by Gruber et al. (1996) meant a leap forward in the back-calculation technique, albeit with certain caveats (Matsumoto and Gruber, 2005). The C_{ant} was then accordingly re-expressed as the difference between the quasi-conservative tracer $\Delta C^* = (C_{\text{T}}^{\circ} - C_{\text{Teq}}^{\pi})$ and $\Delta C_{\text{dis}}^{\pi}$ (C_{T}^{π} is the C_{T} in equilibrium with the preindustrial atmospheric CO₂ level of 280 ppm).

The current paper examines some of the above outlined shortcomings that are habitual in C_{ant} back-calculation approaches and proposes some upgrades to them. Special emphasis is placed on assessing the adequacy of the water column region used to reconstruct WMF conditions at large ocean basin scales. Then accordingly, new parameterizations of A_{T}° and ΔC_{dis} are proposed and their long-term variability are given consideration. Finally, the impact of the proposed methodology modifications on previous Atlantic C_{ant} inventory estimates is also addressed.

2 Dataset

The Atlantic Ocean plays a leading role in the thermohaline circulation context given the numerous deep-water mass formation processes it hosts and it has been selected as an optimal test-bed for the proposed C_{ant} estimation modifications. In total, ten selected cruises to give representative Atlantic coverage were used (Fig. 1 and Table 1). These include the WOCE tracks A02, A14, A16, A17, A20, AR01, I06-Sa and I06-Sb, the CLIVAR A16N legs 1 and 2, the WOCE/CLIVAR OVIDE 2002 and 2004 cruises and the NSeas-Knorr cruise (Bellerby et al., 2005; Olsen et al., 2006). The availability of high-quality carbon system measurements, calibrated with Certified Reference Materials (CRMs), was one of the heavyweight cruise selection criteria. All of the above cruises are part of the Atlantic Synthesis effort made within the CARBOOCEAN Integrated Project framework (<http://www.carbon-synthesis.org/>). The data are available from the Global Ocean Data Analysis Project (GLODAP; http://cdiac.ornl.gov/oceans/glodap/Glodap_home.htm), the Climate Variability and Pre-

BGD

6, 4527–4571, 2009

Anthropogenic CO₂ in the Atlantic Ocean

M. Vázquez-Rodríguez
et al.

Title Page

Abstract

Introduction

Conclusions

References

Tables

Figures

◀

▶

◀

▶

Back

Close

Full Screen / Esc

Printer-friendly Version

Interactive Discussion



dictability (CLIVAR; <http://www.clivar.org>) and the Carbon In the Atlantic (CARINA; <http://store.pangaea.de/Projects/CARBOOCEAN/carina/index.htm>) data portals.

For the vast majority of the samples, pressure and temperature data come from filtered CTD measurements. Salinity and nutrient data come from analysis of individual Niskin bottles collected with a rosette. All WOCE C_T samples kept in the current dataset were analyzed with the coulometric titration technique. The OVIDE cruise C_T data was obtained from thermodynamic equations using pH and A_T direct measurements and the carbon dioxide dissociation constants from Dickson and Millero (1987). All shipboard A_T measurements were analysed by potentiometric titration using a titration system and a potentiometer, and further determined by either developing a full titration curve (Millero et al., 1993; DOE, 1994; Ono et al., 1998) or by single point titration (Pérez and Fraga, 1987; Mintrop et al., 2002). The pH measurements were determined using pH electrodes or, more commonly, with a spectrophotometric method (Clayton and Byrne, 1993) adding *m*-cresol purple as the indicator in either scanning or diode array spectrophotometers. Analytical accuracies of C_T , A_T and pH are typically assessed within $\pm 2 \mu\text{mol kg}^{-1}$, $\pm 4 \mu\text{mol kg}^{-1}$ and ± 0.003 pH units, respectively. A downward adjustment of $8 \mu\text{mol kg}^{-1}$ in the A_T values from WOCE A17 (Table 1) has been suggested by Ríos et al. (2005) after comparing A_T data from that cruise with other measurements. Otherwise, the preliminary results from a crossover analysis exercise performed by the CARBOOCEAN Atlantic Synthesis group sustain that no further corrections are needed for the carbon system parameters of the selected cruises.

BGD

6, 4527–4571, 2009

Anthropogenic CO₂ in the Atlantic Ocean

M. Vázquez-Rodríguez
et al.

Title Page

Abstract

Introduction

Conclusions

References

Tables

Figures

◀

▶

◀

▶

Back

Close

Full Screen / Esc

Printer-friendly Version

Interactive Discussion



3 Method

3.1 The subsurface layer reference for reconstructing water mass formation conditions

It is not until water masses are rapidly capped by the seasonal thermocline and loose contact with the atmosphere that the degrees of O₂ and CO₂ air-sea disequilibria are established and preformed properties are defined. Therefore, any data (but specially surface) collected during this time befalls of incontrovertible value if one is to estimate C_{ant} and infer from such measurements the ΔC_{dis} or any carbon system preformed property, most importantly A_T^o and C_T^o. The surface outcropping of water masses is most common in high Atlantic latitudes and typically occurs towards late wintertime. This is the time when minimum seasonal values of temperature, minimum annual air-sea and water column vertical pCO₂ gradients and maximum thickness of winter mixed layers are reached. Unfortunately, the harsh meteorological conditions and the extension of ice covers at high latitudes diminish the number of cruises that can be conducted, making late wintertime surface data scarcely available and providing only sparse spatial coverage. On the contrary and to our profit, the subsurface layer has the advantage of retaining these wintertime WMF conditions quite stable up to sixth months after, when cruises are normally executed.

The surface ocean seasonal cycle has a large sea surface temperature (SST), C_T and pCO₂ variability (Bates et al., 1996; Corbière et al., 2007). Typical SST oscillations can reach up to 10°C (Pond and Pickard, 1993) in temperate waters and up to 6°C in subpolar regions where WMF processes abound (Lab Sea Group, 1998). In the case of pCO₂, the amplitude of variations ranges between 80 and 160 ppm, which in last instance translates into significant changes of surface C_T (Bates et al., 1996; Lefèvre et al., 2004; Lüger, 2004; Corbière et al., 2007). Given such variability the use of surface measurements becomes dubious, even in the case of conservative parameters like θ , S, NO or PO (Broecker, 1974) for parameterizations that aim to characterize outcrop events and their associated WMF conditions. Its use would inevitably lead to

Anthropogenic CO₂ in the Atlantic Ocean

M. Vázquez-Rodríguez
et al.

Title Page

Abstract

Introduction

Conclusions

References

Tables

Figures

◀

▶

◀

▶

Back

Close

Full Screen / Esc

Printer-friendly Version

Interactive Discussion



reconstructing a manifold of plausible but inaccurate WMF scenarios depending on the sampling date of surface data (Lo Monaco et al., 2005).

As an alternative to the often unavailable surface late wintertime data Pérez et al. (2002) and Ríos et al. (2003) used regional data from the 50–200 m layer as a first approximation to the winter mixed layer preformed conditions. It can be easily checked from any climatological database (the World Ocean Atlas 2005-WOA05, for example) how from January through April (typically) surface and subsurface tracer concentrations are more alike than during the rest of the year. Most remarkably, the physical and biological forcing of conservative tracer concentrations in the subsurface layer (100–200 m from hereon) is at least one order or magnitude less than in the case of the surface layer. This means that WMF properties are longer preserved throughout the annual cycle in the 100–200 m domain. Adding to the above arguments, the thermohaline variability of the ocean interior and the subsurface layer are very much alike (Fig. 2). The latter tightly encloses and represents the assortment of water masses existing in the bulk of the Atlantic Ocean, unlike the uppermost 25 m of surface waters. One final and mostly pragmatic aspect yet to relying on subsurface data to recreate WMF conditions is that it greatly reduces the sparseness of data available for parameterizations compared to wintertime surface data.

3.2 Estimation of A_T° in the subsurface layer

Several A_T° parameterizations have been previously proposed, like the ones from Gruber et al. (1996) or Millero et al. (1998), based on surface A_T observations gathered normally during the summer or spring. It has been shown by other authors that these parameterizations yield systematic negative $\Delta A_T = A_T - A_T^\circ$ values despite of the net increases of silicate observed in the area where the equations were applied (Broecker and Peng, 1982; Ríos et al., 1995; Pérez et al., 2002). We now investigate how considering different variables and using subsurface data can improve the estimation of A_T° .

From the selected cruises (Fig. 1), the latitudinal distributions in the subsurface layer

BGD

6, 4527–4571, 2009

Anthropogenic CO₂ in the Atlantic Ocean

M. Vázquez-Rodríguez et al.

Title Page

Abstract

Introduction

Conclusions

References

Tables

Figures

◀

▶

◀

▶

Back

Close

Full Screen / Esc

Printer-friendly Version

Interactive Discussion



Anthropogenic CO₂ in the Atlantic Ocean

M. Vázquez-Rodríguez
et al.

Title Page

Abstract

Introduction

Conclusions

References

Tables

Figures

◀

▶

◀

▶

Back

Close

Full Screen / Esc

Printer-friendly Version

Interactive Discussion



of θ , S, silicate, water mass age (from CFC12), normalized (to salinity 35) potential A_T (NPA_T) and ΔC_{dis} are displayed in Fig. 3. The normalization of A_T to $S=35$ has been traditionally used to compensate freshwater balance effects (Friis, 2006) and transform all surface waters close to subsurface conditions. The potential A_T (PA_T) term is defined as $PA_T = A_T + NO_3 + PO_4$, after Brewer et al. (1975) and Fraga and Álvarez-Salgado (2005). The main advantage of including PA_T instead of A_T in parameterizations is that organic matter remineralization has no effect on PA_T . However, PA_T remains to be a valid alkalinity shift indicator because it is still affected by $CaCO_3$ dissolution (by a factor of two). One highlight of the distributions in Fig. 3 is how the strong NPA_T and silicate gradients at about 50° S match together and draw a clear line of demarcation between waters with strong Antarctic influence and the rest. Taking into account the existing relationship between silicate and A_T that stems from the dissolution of opal and calcium carbonate (from Fig. 3, the NPA_T vs. silicate linear fit has a $R^2=0.88$) described in Pérez et al. (2002), silicate is introduced in the following PA_T parameterization:

$$PA_T \pm 4.6 = 585.7 \pm 13 + (46.2 \pm 0.4)S + (3.27 \pm 0.07)\theta + (0.240 \pm 0.005)NO + (0.73 \pm 0.01)Si \quad (R^2=0.97, n=1951) \quad (1)$$

Where $NO=9NO_3+O_2$ ($\mu\text{mol kg}^{-1}$) is the conservative tracer defined by Broecker (1974), and Si is the silicate concentration ($\mu\text{mol kg}^{-1}$). Since this PA_T equation has been obtained using subsurface data, the approximation $PA_T \approx PA_T^\circ$ can be soundly made, as the used data subset represents best the moment of WMF. Thus, from Eq. (1): $A_T^\circ = PA_T - (NO_3^\circ + PO_4^\circ)$, where $NO_3^\circ = NO_3 - AOU/9$ and $PO_4^\circ = PO_4 - AOU/135$. AOU stands for Apparent Oxygen Utilization. The $O_2:N=9$ and $O_2:P=135$ Redfield ratios here used were proposed by Broecker (1974). These remineralization ratios have been satisfactorily applied previously in C_{ant} determination by Pérez et al. (2002) in the North Atlantic region. The error of the fit from Eq. (1) has been evaluated in terms of $CaCO_3$ dissolution (ΔCa), since $\Delta Ca = 0.5(PA_{T,observed} - PA_T^\circ)$, and is estimated within $\pm 4.6 \mu\text{mol kg}^{-1}$, which is lower than the errors reported in Gruber et al. (1996) and in

3.3 On the temporal variability of A_T°

The well-documented processes of rising sea surface temperature (SST), ocean acidification and changes in CaCO_3 dissolution over the last two centuries come to challenge the now commonly accepted temporal invariability of the A_T° term. Such processes must be discussed and accounted for in A_T° estimates.

The dissolution of calcium carbonate (CaCO_3) neutralizes C_{ant} and adds A_T via the dissolution reaction: $\text{CO}_2 + \text{CaCO}_3 + \text{H}_2\text{O} \rightarrow 2\text{HCO}_3^- + \text{Ca}^{2+}$. Such A_T increase would enhance the buffering capacity of seawater (Harvey, 1969), allowing for an even larger atmospheric CO_2 absorption. However, the current rise of the atmospheric CO_2 levels has also lessened the activity of calcifying organisms in surface waters and increased the C_T/A_T ratio, causing an upward translation of the aragonite saturation horizon (Riebesell et al., 2000; Sarma et al., 2002; Heinze, 2004). As these processes unfold over time they alter the value of preformed A_T in the newly formed water masses. In spite of the buffering capacity of the ocean to quench excess CO_2 , a sustained increase of atmospheric $p\text{CO}_2$ will lead to a large-scale acidification of the ocean that is more readily sensed by the uppermost layers of the ocean, including subsurface. The lowering of seawater pH may have severe consequences for marine biota, especially for those organisms that incorporate carbonate to their exoskeletons and other biomechanical structures (Royal Society, 2005). Heinze (2004) has performed a model scenario for the change in global marine biogenic CaCO_3 export production derived from the increasing anthropogenic fraction of atmospheric CO_2 . His laboratory findings were extrapolated to the world ocean using a 3-D ocean general circulation model (OGCM) and the results point to a decrease of 50% in the biological CaCO_3 export production by year 2250 for an assumed A1B IPCC emission scenario ($x\text{CO}_2$ of 1400 ppm). This result translates into a ~5% decrease ($-0.03 \text{ Gt-C CaCO}_3 \text{ yr}^{-1}$) in the biogenic CaCO_3 export production that would be taking place nowadays. Also, this would pro-

Anthropogenic CO_2 in the Atlantic Ocean

M. Vázquez-Rodríguez
et al.

Title Page

Abstract

Introduction

Conclusions

References

Tables

Figures

◀

▶

◀

▶

Back

Close

Full Screen / Esc

Printer-friendly Version

Interactive Discussion



voke a modest sustained increase of surface alkalinity that would have developed over the last two centuries. Such increase can represent up to 5% of the present C_{ant} signal in any given sample, i.e., a $2.1 \mu\text{mol kg}^{-1}$ bias in water parcels saturated of C_{ant} under the present atmospheric $x\text{CO}_2$.

5 On the other hand, a global average increase in SST of $1.8\text{--}2.0^\circ\text{C}$ has been reported for the North Atlantic (Rosenheim et al., 2005). Depending on the author this amount varies from 0.8 to 2.0°C (Levitus et al., 2001; Curry et al., 2003; IPCC, 2007). The changes in the upper ocean temperature due to global warming would not have an effect on the NPA_T due to thermal dependant biogeochemical processes. The hydro-
10 logical balance affects salinity and alkalinity evenly, meaning that the long time scale salinity shifts in the surface layer do not affect the alkalinity/salinity ratio, i.e., NPA_T . In spite of it, using present day θ data in Eq. (1) can bias the estimates of preindustrial A_T° since any considered water mass would have formed under different values of θ back then in history. At the present day, the NPA_T shows a positive rate of increase
15 polewards with respect to SST of $-4 \mu\text{mol kg}^{-1} \text{ }^\circ\text{C}^{-1}$ (from data in Fig. 3a and e). Accordingly, if Eq. (1) was to be applied to make historical estimates of A_T° using present day values of θ , overestimates in NPA_T of $\sim 4 \mu\text{mol kg}^{-1}$ could be introduced.

The decrease of preindustrial A_T° due to CaCO_3 dissolution changes and SST shifts was corrected in our calculations according to the expression $\text{PA}_T^\circ = \text{NPA}_T^\circ - (0.1 C_{\text{ant}}^{\text{sat}} + 4)$.
20 Here, $C_{\text{ant}}^{\text{sat}}$ stands for the theoretical saturation concentration of C_{ant} of the sample, which mostly depends on the atmospheric $p\text{CO}_2$ to which the water mass was exposed during its time of formation. Since we are attempting to quantify the temporal variability of A_T° , the $C_{\text{ant}}^{\text{sat}}$ was used to account for the acidification effects in the above fit because this variable is $p\text{CO}_2$ and, therefore, time dependant. The impact of the combined effects of ocean acidification and SST increase is big enough to be significant in
25 terms of C_{ant} inventory. However, their influence is lower than the uncertainty in C_{ant} determination (normally around $\pm 5 \mu\text{mol kg}^{-1}$, depending on the estimation method). These minor corrections would be very difficult to quantify directly through measure-

**Anthropogenic CO_2
in the Atlantic Ocean**M. Vázquez-Rodríguez
et al.

Title Page

Abstract

Introduction

Conclusions

References

Tables

Figures

◀

▶

◀

▶

Back

Close

Full Screen / Esc

Printer-friendly Version

Interactive Discussion



ments, but they should still be considered if a maximum $4 \mu\text{mol kg}^{-1}$ bias ($2 \mu\text{mol kg}^{-1}$ on average) in C_{ant} estimates wants to be avoided.

Figures 4a and 4b show the ΔCa calculated using the A_{T}° proposed by Lee et al. (2003) (which it is practically coincident with Gruber et al., 1996) and the A_{T}° from Eq. (1). The distribution trends and values of both parameterizations are highly correlated ($R^2=0.77$, $n=4923$). The ΔCa distributions agree on the accumulation of calcium and increasing alkalinity in deep waters, mainly in the Deep South Atlantic where the oldest water masses are found. However, there is still a significant offset in the ΔCa fields of $11 \mu\text{mol kg}^{-1}$. The A_{T}° equation from Lee et al. (2003) produces negative ΔCa in most of the North Atlantic south of its application range limit (latitude $<60^{\circ}\text{N}$). Negative values of ΔCa up to $-17 \mu\text{mol kg}^{-1}$ are reached, indicating that there is CaCO_3 precipitation in those areas. Nonetheless, there is no evidence that such net precipitation of CaCO_3 predominates over dissolution below the subsurface layer. The review of the global carbonate budget (Milliman et al., 1999; Berelson et al., 2007) shows that a considerable portion of surface-produced calcite (as much as 60–80%) dissolves in the upper 1000 m, above the lysocline, as a result of biological mediation. It has been previously demonstrated by other authors how even though the upper ocean is supersaturated with CaCO_3 , there is a downward increase of the CaCO_3 dissolution (Broecker and Peng, 1982). Additionally, data from sediment traps in the North Atlantic corroborates the dissolution of CaCO_3 in the upper layers of this ocean (Honjo and Manganini, 1993; Martin et al., 1993). The A_{T}° parameterization from this study has satisfactorily produced positive ΔCa values in the whole Atlantic and low ΔCa in the Nordic Seas.

3.4 Estimation of ΔC_{dis} in the subsurface layer

The disequilibrium between the rapidly increasing atmospheric $p\text{CO}_2$ and the sea surface $p\text{CO}_2$ largely determines the behaviour of the ocean as a CO_2 source or sink. The increasing net uptake of CO_2 by the ocean at a global scale is sustained by an increas-

BGD

6, 4527–4571, 2009

Anthropogenic CO_2 in the Atlantic Ocean

M. Vázquez-Rodríguez
et al.

Title Page

Abstract

Introduction

Conclusions

References

Tables

Figures

◀

▶

◀

▶

Back

Close

Full Screen / Esc

Printer-friendly Version

Interactive Discussion



Anthropogenic CO₂ in the Atlantic Ocean

M. Vázquez-Rodríguez
et al.

Title Page

Abstract

Introduction

Conclusions

References

Tables

Figures

◀

▶

◀

▶

Back

Close

Full Screen / Esc

Printer-friendly Version

Interactive Discussion



ing air-sea $p\text{CO}_2$ gradient. The ΔC_{dis} can not be measured directly like in the case of A_T and must therefore be defined theoretically from observable parameters. The present-day ΔC_{dis} (ΔC_{dis}^t) term was first estimated in the context of C_{ant} determination by Gruber et al. (1996), who defined it conceptually as the difference between the C_T in the mixed layer at the time of WMF ($C_T^{\circ t}$) and the theoretical C_T in equilibrium with the corresponding atmospheric $p\text{CO}_2$ ($C_{T\text{eq}}^t$). We applied this definition (Eq. 2) to the subset of subsurface data from our selected cruises (Fig. 3f). To obtain $C_T^{\circ t}$, the measured C_T in the described subsurface layer must be corrected for the organic matter remineralization and ΔCa contributions. The $C_{T\text{eq}}^t$ term is obtained from thermodynamic equations using subsurface measurements of S , θ , nutrients, AOU, A_T° and age estimated from CFC12 concentrations. The water pressure and fugacity terms have been taken into account in the calculation of $C_{T\text{eq}}^t$ (Pérez et al., 2002). The PA_T° term was calculated applying Eq. (1).

$$\Delta C_{\text{dis}}^t = C_T^{\circ t} - C_{T\text{eq}}^t = C_T - (\text{AOU}/R_C + 0.5(\text{PA}_T - \text{PA}_T^{\circ})) - C_{T\text{eq}}^t(x\text{CO}_2(t), A_T^{\circ}, S, \theta) \quad (2)$$

Given this definition, positive ΔC_{dis} values represent sea outgasing of CO_2 and negative values indicate CO_2 uptake by the ocean. The subsurface ΔC_{dis} distribution in Fig. 3f resembles very much the one derived from the $p\text{CO}_2$ climatology of Takahashi et al. (2002) except for the high latitude areas, where the climatology lacks data (especially during wintertime).

The shortcoming of the ΔC_{dis}^t definition in Eq. (2) is its dependence on non-conservative tracers, which is a compulsory and desirable feature in any robust parameterization of oceanographic variables. Hence, the estimated subsurface ΔC_{dis} data (Fig. 3f) are used as input to construct a multilinear regression (MLR) model that uses only conservative variables. The obtained fit is given in Eq. (3). The specific parametric coefficients of equation for different temperature and latitude intervals are summarised in Table 2, together with the error estimates of the model.

$$\Delta C_{\text{dis}}^t = a + b(\theta - 10) + c(S - 35) + d(\text{NO} - 300) + e(\text{PO} - 300) \quad (3)$$

For the case of Central Waters ($8 \leq \theta \leq 18^\circ\text{C}$) a distinction between hemispheres has been made because no mixing between Arctic and Antarctic waters takes place in this oceanographic region. It is therefore possible to calculate ΔC_{dis} more accurately through specific equations from the northern and southern hemispheres. In the Equatorial Upwelling region a thermal threshold between warm ($\theta > 18^\circ\text{C}$) subsurface waters and colder waters has been also established. The fitted ΔC_{dis} shows a high correlation with the original values calculated using Eq. (2) ($R^2 = 0.72$; $n = 1934$). The uncertainties for the ΔC_{dis} values obtained using conservative variables in Eq. (3) are between 4 and $7 \mu\text{mol kg}^{-1}$ (average $5.6 \mu\text{mol kg}^{-1}$; Table 2).

3.5 On the temporal variability of ΔC_{dis} ($\Delta\Delta C_{\text{dis}}$)

Ever since it was first introduced in the C_{ant} back-calculation equations by Gruber et al. (1996) the main assumption regarding ΔC_{dis} has been its invariability over time ($\Delta C_{\text{dis}}^\pi = \Delta C_{\text{dis}}^t$, where “ π ” stands for preindustrial) for a given oceanic region (Gruber et al., 1996; Gruber, 1998; Wanninkhof et al., 1999; Lee et al., 2003). Conversely, according to Sabine et al. (2004), the C_{ant} inventory is estimated to have a present annual rate of increase of $1.8 \pm 0.4 \text{ Pg C yr}^{-1}$. Such C_{ant} uptake and inventory increase is sustained by the increasing air-sea $p\text{CO}_2$ gradient. This means that the atmospheric $p\text{CO}_2$ increases faster than the uptake mechanisms of the ocean can cope with on a yearly basis. This result makes the assumption of invariable ΔC_{dis} rather imprecise (Hall et al., 2004; Matsumoto and Gruber, 2005).

The effects of the temporal variation of ΔC_{dis} ($\Delta\Delta C_{\text{dis}} = \Delta C_{\text{dis}}^t - \Delta C_{\text{dis}}^\pi$) on the inventories of C_{ant} have been recently evaluated in Matsumoto and Gruber (2005). A rate of increase of $1.8 \pm 0.4 \text{ Pg C yr}^{-1}$ (Sabine et al., 2004) would produce an annual increase on the average oceanic C_{ant} specific inventory of $0.46 \text{ mol C m}^{-2} \text{ yr}^{-1}$. Knowing that the globally averaged gas exchange coefficient for CO_2 is $\sim 0.052 \pm 0.015 \text{ mol C m}^{-2} \text{ yr}^{-1} \mu\text{atm}^{-1}$ (Naegler et al., 2006), implies that the global average air-sea $\Delta f\text{CO}_2$ induced by the anthropogenic CO_2 fraction would

Anthropogenic CO_2 in the Atlantic Ocean

M. Vázquez-Rodríguez
et al.

[Title Page](#)[Abstract](#)[Introduction](#)[Conclusions](#)[References](#)[Tables](#)[Figures](#)[◀](#)[▶](#)[◀](#)[▶](#)[Back](#)[Close](#)[Full Screen / Esc](#)[Printer-friendly Version](#)[Interactive Discussion](#)

amount up to $-8.0 \mu\text{atm}$ (see Fig. 1 in Biastoch et al., 2007). As estimated by Matsumoto and Gruber (2005) this would correspond to a theoretical average $\Delta\Delta C_{\text{dis}}$ of $-5.0 \pm 1.0 \mu\text{mol kg}^{-1}$ that would have developed since the preindustrial era. Accordingly, these authors have suggested a -7% correction factor to the ΔC^* estimated C_{ant} inventories in Lee et al. (2003) and Sabine et al. (2004).

Matsumoto and Gruber (2005) have proposed a model for the temporal evolution of ΔC_{dis} (see their Fig. 2). On their Eq. (5) a formal relationship between $\Delta\Delta C_{\text{dis}}$ and C_{ant} is given, namely: $\Delta\Delta C_{\text{dis}} = \beta/k_{\text{ex}} C_{\text{ant}}$. The term k_{ex} is the globally averaged air-sea gas exchange coefficient for CO_2 ($0.065 \pm 0.015 \text{ mol C m}^{-2} \text{ yr}^{-1} \mu\text{atm}^{-1}$ according to Broecker et al., 1985). The β is a constant factor that they estimate ($0.0065 \pm 0.0012 \text{ mol C m}^{-2} \text{ yr}^{-1} \mu\text{atm}^{-1}$) from the constraint that the global C_{ant} uptake flux integrated over the industrial period must equal the total inventory of anthropogenic CO_2 in the ocean. Hence, the overall proportionality factor between $\Delta\Delta C_{\text{dis}}$ and C_{ant} they obtain is $\beta/k_{\text{ex}} \approx 0.1$.

Observations indicate that ΔC_{dis} varies spatially due to the rapid uptake capacity and solubility changes governed mainly by temperature and wind speed, the biological pump and the vertical mixing. The dilution of transient tracers, in particular C_{ant} and CFCs above the seasonal thermocline strongly depends on the winter mixed layer depth (WMLD) (Doney and Jenkins, 1988). On the subtropical regions, where WMLD is shallow ($\sim 100\text{--}200 \text{ m}$), the average C_{ant} content is close to saturation ($\sim 60 \mu\text{mol kg}^{-1}$). Applying Eq. (5) from Matsumoto and Gruber (2005) would yield a $\Delta\Delta C_{\text{dis}} \approx -6 \mu\text{mol kg}^{-1}$. Likewise, subpolar regions with WMLD of $\sim 500 \text{ m}$ or larger have average C_{ant} concentrations of $\sim 40 \mu\text{mol kg}^{-1}$. The estimated $\Delta\Delta C_{\text{dis}}$ as of Matsumoto and Gruber (2005) would be of $-4 \mu\text{mol kg}^{-1}$. However, model-derived synthetic data given in Fig. 8b from Matsumoto and Gruber (2005) yield estimates of $\Delta\Delta C_{\text{dis}} \approx 0$ and $-10 \mu\text{mol kg}^{-1}$ for the subtropical areas and subpolar areas, respectively. These contradictions suggest that the proportionality factor β/k_{ex} should not be constant. Matsumoto and Gruber (2005) have acknowledged the effects of their approximation and have indicated a possible improvement for it: β/k_{ex} could be deter-

Anthropogenic CO_2 in the Atlantic Ocean

M. Vázquez-Rodríguez et al.

Title Page

Abstract

Introduction

Conclusions

References

Tables

Figures

◀

▶

◀

▶

Back

Close

Full Screen / Esc

Printer-friendly Version

Interactive Discussion



Anthropogenic CO₂ in the Atlantic Ocean

M. Vázquez-Rodríguez
et al.

Title Page

Abstract

Introduction

Conclusions

References

Tables

Figures

◀

▶

◀

▶

Back

Close

Full Screen / Esc

Printer-friendly Version

Interactive Discussion



mined for different regions by applying the integral constraint to individual isopycnals in order to obtain regional β and by determining the corresponding regional k_{ex} . Next, we propose a simpler method to account for the horizontal (spatial) and vertical (temporal) variability of the β/k_{ex} factor in the area under study. This should provide a correction for the positive bias linked to $\Delta\Delta C_{\text{dis}}$.

The magnitude of $\Delta\Delta C_{\text{dis}}$ is assumed to be controlled by the interactions of wind speed, ocean circulation and surface ocean buffering particularly in regions where strong subsurface mixing processes occur. Based on the $\Delta p\text{CO}_2$ climatology from Takahashi et al. (2002) it can be stated that the absolute values of $\Delta\Delta C_{\text{dis}}$ ($|\Delta\Delta C_{\text{dis}}|$) and ΔC_{dis} ($|\Delta C_{\text{dis}}|$) co-variate with WMLD except in Equatorial warm surface waters. This empirical result provides a simple process-based argument for trying to express β/k_{ex} as a function of the WMLD and, in so doing, relaxing the assumption of constant β/k_{ex} . Regions with thick WMLs need longer time periods (several years) to equilibrate and therefore tend to have larger interannual disequilibria (no matter whether in the present or in the preindustrial era) (Azetsu-Scott et al., 2003; Fine et al., 2002; Takahashi et al., 2002). Consequently, $|\Delta\Delta C_{\text{dis}}|$ will tend toward larger values on areas with large $|\Delta C_{\text{dis}}|$. To a lesser extent than in the high latitudes, the Equator has an anti-correlation between $\Delta\Delta C_{\text{dis}}$ and $f\text{CO}_2$, i.e., it displays negative $\Delta\Delta C_{\text{dis}}$ (Matsumoto and Gruber, 2005) and high sea surface $f\text{CO}_2$ values (Takahashi et al., 2002). Knowing of this exception and given the above argumentation, even if a coarse correlation between the $\Delta\Delta C_{\text{dis}}$ and ΔC_{dis} is assumed, Eq. (5) in Matsumoto and Gruber (2005) can be re-expressed and re-fitted in terms of C_{ant} and $\Delta C_{\text{dis}}^{\text{t}}$ (Eq. 4) to account for the variability of β/k_{ex} .

$$\Delta\Delta C_{\text{dis}} = -\varphi \left(C_{\text{ant}} / C_{\text{ant}}^{\text{sat}} \right) |\Delta C_{\text{dis}}^{\text{t}}| \quad (4)$$

Furthermore, from Eq. (4):

$$\Delta C_{\text{dis}}^{\pi} = \Delta C_{\text{dis}}^{\text{t}} - \Delta\Delta C_{\text{dis}} = \Delta C_{\text{dis}}^{\text{t}} + \varphi \left(C_{\text{ant}} / C_{\text{ant}}^{\text{sat}} \right) |\Delta C_{\text{dis}}^{\text{t}}| \quad (5)$$

The term of C_{ant} saturation ($C_{\text{ant}}^{\text{sat}} = S/35(0.85\theta + 46.0)$), referenced to 4541

Anthropogenic CO₂ in the Atlantic Ocean

M. Vázquez-Rodríguez
et al.

Title Page

Abstract

Introduction

Conclusions

References

Tables

Figures

◀

▶

◀

▶

Back

Close

Full Screen / Esc

Printer-friendly Version

Interactive Discussion



a $x\text{CO}_{2\text{air}}=375$ ppm) is a correction factor that is included to account for the effects of temperature and salinity on the solubility of C_{ant} in the different water masses. The constant term “ φ ” is a proportionality factor and equals the $\Delta\Delta C_{\text{dis}}/\Delta C_{\text{dis}}^{\text{t}}$ ratio. For simplicity, it has been assumed that “ φ ” is constant elsewhere from the Equator.

The Equator is an upwelling region that behaves as a CO₂ source and “ φ ” is assumed to have a positive sign here. Otherwise, the second term in Eq. (4) warrants that $\Delta\Delta C_{\text{dis}}$ will be assigned low values in low latitudes (where C_{ant} is high and $\Delta C_{\text{dis}}^{\text{t}}$ is low). The $C_{\text{ant}}/C_{\text{ant}}^{\text{sat}}$ ratio in Eq. (4) accounts for the temporal variability of $\Delta\Delta C_{\text{dis}}$ (Fig. 2 and Eq. (5) in Matsumoto and Gruber, 2005) that stems from the fact that C_{ant} increases over time forced by the rising atmospheric CO₂ loads. Hence, the $C_{\text{ant}}/C_{\text{ant}}^{\text{sat}}$ ratio represents the degree of equilibrium between the C_{T} in a given sample and the atmospheric CO₂ concentration at the moment of sampling. This implies that the larger the C_{ant} burden of the water mass is, the larger its $\Delta\Delta C_{\text{dis}}$ will be.

The value of the constant proportionality factor “ φ ” in Eq. (4) can be calculated using subsurface estimates given that the air-sea CO₂ disequilibrium is established in the upper ocean layers. To estimate it, the subsurface $\Delta C_{\text{dis}}^{\text{t}}$ for the Atlantic is calculated applying Eq. (3) using hydrographical data from the selected cruises that span over a decade (1993–2003) (Fig. 1, Table 1). By averaging the time interval covered in the dataset we get $t \approx 1998$ and, therefore, $\Delta C_{\text{dis}}^{\text{t}} = \Delta C_{\text{dis}}^{1998}$ in the present study. Next, the C_{ant} in Eq. (4) is calculated for subsurface waters applying the CFC-age “shortcut” method with CFC12 data (Thomas and Ittekkot, 2001). The average age of the water masses in the Atlantic subsurface layer, including the important outcropping regions, is under 25 years (Fig. 3d). According to Matear et al. (2003), the use of the shortcut method to estimate C_{ant} is suitable in the case of such young waters in the upper ocean layers. Anyhow, the shortcut method is only applied in the present study in this step of estimating “ φ ”. Lastly, we take an average $\Delta\Delta C_{\text{dis}}$ value for the Atlantic of $-5.0 \pm 1.0 \mu\text{mol kg}^{-1}$ (Matsumoto and Gruber, 2005) and calculate the mean of Atlantic subsurface estimates for the “ $C_{\text{ant}}/C_{\text{ant}}^{\text{sat}}|\Delta C_{\text{dis}}^{\text{t}}|$ ” part in Eq. (4) ($-9.5 \pm 0.3 \mu\text{mol kg}^{-1}$ is obtained). Considering the above calculations, a value of $\varphi = 0.55 \pm 0.10$ is finally

achieved.

Alternatively, taking this value of φ and applying it in Eq. (5) yields an average $\Delta C_{\text{dis}}^{\pi} = -4.5 \mu\text{mol kg}^{-1}$ for the Atlantic. This corollary result indicates that during the preindustrial era the average ΔC_{dis} was, on average, less negative than at present. For comparison, Matsumoto and Gruber (2005) obtained average values of $\Delta\Delta C_{\text{dis}} = -5.5 \mu\text{mol kg}^{-1}$ and $\Delta C_{\text{dis}}^{\pi} = -7.0 \mu\text{mol kg}^{-1}$ for the global ocean using synthetic surface data from a 3-D OGCM output.

3.6 Modified formulation to estimate C_{ant}

The anthropogenic fraction of C_T is traditionally expressed in the back-calculation context as:

$$C_{\text{ant}} = C_T^{\circ t} - C_T^{\circ \pi} \quad (6)$$

Where:

$$C_T^{\circ t} = C_T - \text{AOU}/R_C - 0.5(\text{PA}_T - \text{PA}_T^{\circ}) = C_T - \text{AOU}/R_C - \Delta\text{Ca} \quad (7)$$

$$C_T^{\circ \pi} = C_{T\text{eq}}^{\pi} + \Delta C_{\text{dis}}^{\pi} \quad (8)$$

All terms in Eq. (7) are calculated directly from hydrographical data. In the case of PA_T° , it is calculated using Eq. (1) and applying the proposed A_T° correction for CaCO_3 dissolution changes and temperature shifts (Sect. 3.3). Then, by substituting Eqs. (7) and (8) into Eq. (6) we get:

$$C_{\text{ant}} = C_T - \text{AOU}/R_C - \Delta\text{Ca} - C_{T\text{eq}}^{\pi} - \Delta C_{\text{dis}}^{\pi} = \Delta C^* - \Delta C_{\text{dis}}^{\pi} \quad (9)$$

Finally, by replacing the expression for $\Delta C_{\text{dis}}^{\pi}$ given in Eq. (5) into Eq. (9) and rearranging terms, we obtain a modified back-calculation equation for estimating C_{ant} :

$$C_{\text{ant}} = \frac{\Delta C^* - \Delta C_{\text{dis}}^t}{1 + \varphi \left| \Delta C_{\text{dis}}^t \right| / C_{\text{ant}}^{\text{sat}}} \quad (10)$$

Title Page

Abstract

Introduction

Conclusions

References

Tables

Figures

◀

▶

◀

▶

Back

Close

Full Screen / Esc

Printer-friendly Version

Interactive Discussion



**Anthropogenic CO₂
in the Atlantic Ocean**M. Vázquez-Rodríguez
et al.

The denominator in Eq. (10) is always higher than or equal to one and thus lower C_{ant} estimates than those from the ΔC^* method will be predicted in most cases. This difference in the estimates will be ultimately modulated by the “weight” of the $\Delta C_{\text{dis}}^{\text{t}}$ term. The presented modification in the methodology and, ultimately, in the formulation is expected to have a significant impact in terms of C_{ant} inventory. The addition of the “ φ ” factor alone represents, on average, a $5 \mu\text{mol kg}^{-1}$ decrease in C_{ant} saturated samples. Interestingly, this is in excellent agreement with the average lowering of C_{ant} estimates from the ΔC^* method suggested by Matsumoto and Gruber (2005). From hereon, C_{ant} calculations obtained after applying Eq. (10) will be referred to as “ $\varphi C_{\text{T}}^{\circ}$ method” C_{ant} estimates.

Several in-detail evaluations of the uncertainties attached to C_{ant} estimation with back-calculation approaches have been thoroughly performed in the past (Gruber et al., 1996; Gruber, 1998; Sabine et al., 1999; Wanninkhof et al., 2003; Lee et al., 2003). They all assessed the uncertainty of C_{ant} estimates by propagating random errors over the precision limits of the various measurements required for solving C_{ant} estimation equations. The A_{T}° parameterization here obtained has an associated error that is two times lower than the one proposed by Gruber et al. (1996). In addition, the cruises used to obtain the parameterizations in the present work produced high-quality datasets with the help of improved analytical methodologies and the use of certified reference materials in the carbon system measurements. We have performed a random propagation of the errors associated with the input variables necessary to solve Eq. (10) and have estimated an overall uncertainty of $5.2 \mu\text{mol kg}^{-1}$ for the C_{ant} estimates obtained with the $\varphi C_{\text{T}}^{\circ}$ method. For comparison, the overall estimated C_{ant} uncertainties in Gruber et al. (1996) and Sabine et al. (1999) are 9 and $6 \mu\text{mol kg}^{-1}$, respectively.

Title Page

Abstract

Introduction

Conclusions

References

Tables

Figures

◀

▶

◀

▶

Back

Close

Full Screen / Esc

Printer-friendly Version

Interactive Discussion



3.7 Calculating A_T° and ΔC_{dis} in the water column

To obtain the full-depth A_T° and ΔC_{dis} profiles it is necessary to convey into the ocean interior the A_T° and ΔC_{dis} calculated for the subsurface layer using Eqs. (1) and (3), respectively. As discussed in Sect. 3.1, applying Eqs. (1) and (3) to subsurface data has served so far to identify and establish subsurface A_T° and ΔC_{dis} representatives of each intermediate and deep-water mass present in the thermohaline fields from the selected cruises.

Depending on the temperature of each sample, different approaches are followed in this work to achieve optimum A_T° and ΔC_{dis} estimates in the whole water column. In the case of water samples above the 5°C isopleth, Eqs. (1) and (3) are applied directly to obtain A_T° and ΔC_{dis} , respectively. The correction proposed in Sect. 3.3 for the temporal variability of A_T° is also applied here. For waters with $\theta < 5^\circ\text{C}$, A_T° and ΔC_{dis} are estimated via an extended Optimum Multiparameter (eOMP) analysis (Poole and Tomczak, 1999; Álvarez et al., 2004).

The main reason for this division is to improve the estimates in cold deep waters where complex mixing processes of Arctic and Antarctic origin waters intervene. The intricate interaction of such water masses uplifts the importance (and complication) of mixing in the lower ocean, backing-up the use of an OMP approach. Moreover, the fact that this region represents an enormous volume of the global ocean ($\sim 86\%$) confers waters below the 5°C isotherm the capability of affecting significantly C_{ant} inventories even from potentially small errors in C_{ant} estimates. Consequently, the determination of A_T° and ΔC_{dis} in samples with $\theta < 5^\circ\text{C}$ must be carefully assessed. These are the principal incentives that justify the different procedures used to calculate A_T° and ΔC_{dis} in the upper and lower ocean layers.

The type values of A_T° for the end-members that make up a water sample could still be calculated applying Eq. (1) directly, even in the case of water masses with $\theta < 5^\circ\text{C}$. This is because Eq. (1) is valid for the temperature range of 0 to 20°C (Fig. 3a) and also because the subsurface domain faithfully represents the assortment of water masses

BGD

6, 4527–4571, 2009

Anthropogenic CO_2 in the Atlantic Ocean

M. Vázquez-Rodríguez
et al.

Title Page

Abstract

Introduction

Conclusions

References

Tables

Figures

◀

▶

◀

▶

Back

Close

Full Screen / Esc

Printer-friendly Version

Interactive Discussion



present in the bulk of the Atlantic Ocean (Fig. 2). Even then, if a water parcel is subject to complex mixing processes it is more appropriate (from a mechanistic point of view) to calculate A_T° based on the A_T° of the founding end-members and their specific mixing proportions, rather than from direct application of a parameterization such as Eq. (1).

5 The same reasoning and modus operandi applies for ΔC_{dis} . The minutia followed in this work for both calculation procedures is given in Appendix A.

Lastly, the saline imprint of the Mediterranean Water (MW) in the North Atlantic can induce to wrong calculations when applying Eqs. (1) or (3) directly in waters above the 5°C isotherm. In these particular cases, the ΔC_{dis} and A_T° have to be propagated
10 into the ocean interior by resolving the triangular mix defined by the end-members of Labrador Seawater (LSW), Subpolar Mode Water (SPMW) and MW (Fig. 2). In our selected cruises the samples influenced by MW are located on a wedge of the TS diagram (Fig. 2) that falls outside of the wrapping from subsurface waters. In samples gathered northwards from 15° N and below 400 m depths the above-mentioned mixing
15 triangle is applied to calculate the mixing percentage of MW. The thermohaline and chemical properties of MW are well documented in the literature (Pérez et al., 1993; Álvarez et al., 2005). The A_T° and ΔC_{dis} type values for the SPMW and LSW were calculated from Eqs. (1) and (3), respectively. For the MW end-member these two type values were determined from the mixing percentages of Eastern North Atlantic Central
20 Water (ENACW) and Mediterranean Overflow Water (MOW) in the Gulf of Cádiz. The θ , S, CFC12 and carbon system data used to calculate the A_T° and ΔC_{dis} type values of MOW were sampled in the Strait of Gibraltar and in the Gulf of Cádiz (Rhein and Hinrichsen, 1993; Santana-Casiano et al., 2002).

**Anthropogenic CO₂
in the Atlantic Ocean**M. Vázquez-Rodríguez
et al.

Title Page

Abstract

Introduction

Conclusions

References

Tables

Figures

◀

▶

◀

▶

Back

Close

Full Screen / Esc

Printer-friendly Version

Interactive Discussion

4 Results and discussion

4.1 Anthropogenic CO₂ fields of the Eastern Atlantic basin

As a mean of putting the φC_T° method through the test, the C_{ant} signal is evaluated in a subset of the selected meridional cruises (denoted by star symbols in Fig. 1) that cover the length and are representative of the Eastern Atlantic basin. The obtained results are then compared with previous C_{ant} estimates calculated for the same cruises by Lee et al. (2003) using the classical ΔC^* method (Fig. 5a and b).

The broad C_{ant} distribution patterns are quite similar for both methods, except in the Southern Ocean. In this region of discrepancy south from the Polar Front, Lee et al. (2003) calculate C_{ant} concentrations in the whole water column that are too low compared to the φC_T° estimates. These low ΔC^* estimates are substantiated by Lee et al. (2003) from two arguments, namely: a) the hindrance of air-sea CO₂ exchanges caused by the extension of sea ice; b) the short residence times of the newly formed deep water in this region, which are not long enough for the water body to sequestrate significant amounts of C_{ant} . In spite of these arguments, it is still difficult to justify so extremely low values of C_{ant} , given that significant CFC concentrations have been reported along the continental rise and bottom waters in this region (Orsi et al., 2002; Matear et al., 2003; Waugh et al., 2006). Conversely, such evidence supports the moderately low C_{ant} values of about $13 \pm 2 \mu\text{mol kg}^{-1}$ from the φC_T° method.

To add to the discussion, Lo Monaco et al. (2005) have presented estimates of C_{ant} in the Southern Ocean of $20 \mu\text{mol kg}^{-1}$ on average, which are even higher than the φC_T° values for the bottom samples south of the Antarctic polar front. Lo Monaco et al. (2005) applied a classical back-calculation approach in which the effect of sea-ice on air-sea oxygen equilibrium was considered. In addition, their method implicitly parameterizes the $\Delta \Delta C_{\text{dis}}$ although they consider a homogeneous spatial distribution of it, like for the air-sea O₂ disequilibrium case on ice-covered surface waters. Nevertheless, their C_{ant} distributions along the WOCE I06-Sb line are in very good agreement

BGD

6, 4527–4571, 2009

Anthropogenic CO₂ in the Atlantic Ocean

M. Vázquez-Rodríguez
et al.

Title Page

Abstract

Introduction

Conclusions

References

Tables

Figures

◀

▶

◀

▶

Back

Close

Full Screen / Esc

Printer-friendly Version

Interactive Discussion



with the φC_T° results in Fig. 5a (Vázquez-Rodríguez et al., 2009).

In regions of strong vertical mixing like the Southern Ocean, the back-calculation methods that use deep water masses to establish a $C_{\text{ant}}=0$ baseline can lead to underestimations of the anthropogenic carbon signal because of inappropriate reference choices (Lo Monaco et al., 2005). It is particularly in these regions where the ΔC^* method is known to set unrealistic zero- C_{ant} references (Sabine et al., 1999). A strong vertical mixing of very old, free-CFC waters with well-ventilated, CFC-rich wintertime surface waters constitutes a case study for the non-linear dependence between C_{ant} and CFC-derived ages (Matear et al., 2003; Matsumoto and Gruber, 2005). This non-linearity affects the ΔC_{dis} determination in the ΔC^* method and transfers a positive bias to the ΔC_{dis} of deep isopycnal surfaces in the South Atlantic (Gruber, 1998). The φC_T° method has produced moderately low C_{ant} estimates in the polar and subpolar regions of the section (Southern Ocean and Nordic Seas) mainly due to the influence of the $\Delta \Delta C_{\text{dis}}$ term (Fig. 5c). These estimates stem directly from the high $|\Delta C_{\text{dis}}|$ values found in the Southern Ocean and Nordic Seas at present (Fig. 3f). An important advancement of the φC_T° method in this aspect is that the use of CFCs on the proposed equations is completely unnecessary.

On the other hand, the $|\Delta \Delta C_{\text{dis}}|$ maxima ($-7 \mu\text{mol kg}^{-1}$) are located in the subtropical gyres, where C_{ant} estimates are close to saturation values. This represents a clear discrepancy with model results presented by Matsumoto and Gruber (2005) of approx. $-2 \mu\text{mol kg}^{-1}$ for the same area. Nonetheless, these warm surface waters (above 13°C) represent only $\sim 3.6\%$ of the Atlantic volume and this divergence would yield a minor dissimilarity of 0.023 Gt of C_{ant} in terms of total inventory. Alternatively, the $\Delta \Delta C_{\text{dis}}$ values in the high latitudes are moderate (around 4 and $6 \mu\text{mol kg}^{-1}$ for the Southern Ocean and Nordic Seas, respectively). These results are in good agreement with the surface $\Delta \Delta C_{\text{dis}}$ estimates shown in Matsumoto and Gruber (2005) and will have a remarkable impact in terms of inventory because of the penetration of moderate amounts of C_{ant} in the large volume of the Southern Ocean.

**Anthropogenic CO₂
in the Atlantic Ocean**M. Vázquez-Rodríguez
et al.

Title Page

Abstract

Introduction

Conclusions

References

Tables

Figures

◀

▶

◀

▶

Back

Close

Full Screen / Esc

Printer-friendly Version

Interactive Discussion



4.2 Atlantic inventories of C_{ant}

Although the calculation of a new inventory of C_{ant} is beyond the scope of this study it is still worth discussing the implications of the modifications here proposed. The work from Lee et al. (2003) provides detailed C_{ant} inventories for the Eastern and Western Atlantic basins (Table 5 in Lee et al., 2003) calculated using the ΔC^* method estimates in a large number of WOCE-JGOFS sections. In the present work, the specific inventory of C_{ant} from the $\varphi C_{\text{T}}^{\circ}$ method was calculated without rejecting negative C_{ant} values that were within a 2σ confidence interval of the determination uncertainties ($5.6 \mu\text{mol kg}^{-1}$). After Lee et al. (2003), the average specific inventories were determined with a meridional resolution of 10° for the Eastern Atlantic basin (Fig. 6) using the same cruises as in Sect. 4.1. To make results perfectly comparable with Lee et al. (2003), the studied section was referenced to the WOCE/JGOFS canonical year 1994. This was done using the temporal variation of $C_{\text{ant}}^{\text{sat}}$ as a scaling factor. In addition, the C_{ant} inventories obtained by Gruber (1998) with the ΔC^* for the same region during the middle 1980s were also rescaled and referenced to 1994 so as to include them in Fig. 6.

The C_{ant} inventories from Lee et al. (2003) and the one obtained with the $\varphi C_{\text{T}}^{\circ}$ method are highly correlated ($R^2=0.95$) in the broad 40°S – 30°N latitude band, notwithstanding the fact there exist regions of discrepancy. The calculated specific inventories in the Iceland basin and the Nordic Seas are $\sim 20\%$ and $\sim 40\%$ higher, respectively, than those in Lee et al. (2003) and Gruber et al. (1998). The largest differences in the specific inventory are found in the Nordic Seas and in the Southern Ocean (Fig. 6), as expected from the results in the former section. The $\varphi C_{\text{T}}^{\circ}$ method predicts a specific inventory of C_{ant} for the Southern Ocean of 48 mol C m^{-2} , which is four times higher than the ΔC^* ones in Gruber et al. (1998) and Lee et al. (2003). The C_{ant} method intercomparison work from Vázquez-Rodríguez et al. (2009) shows how different independent methods like the TTD (Waugh et al., 2006) or the TrOCA (Touratier et al., 2007) have also calculated higher inventories than the ΔC^* approach for the same WOCE lines, supporting the $\varphi C_{\text{T}}^{\circ}$ method estimates. On the other end, Lo Monaco et al. (2005) have

BGD

6, 4527–4571, 2009

Anthropogenic CO_2 in the Atlantic Ocean

M. Vázquez-Rodríguez
et al.

Title Page

Abstract

Introduction

Conclusions

References

Tables

Figures

◀

▶

◀

▶

Back

Close

Full Screen / Esc

Printer-friendly Version

Interactive Discussion



reported 58 and 65 mol C m⁻² south from 65° S and between 55° S–64° S, respectively. These estimates are 9 and 16 mol C m⁻² higher than the ones computed with the φC_T° method. Part of these differences can be attributed to the implicitly assumed O₂ equilibrium estate in the φC_T° method and to the $\Delta\Delta C_{\text{dis}}$ approach and fit here proposed (Vázquez-Rodríguez et al., 2009). Also, the φC_T° method does not consider the ΔC_{dis} and A_T° as constant terms, like the method in Lo Monaco et al. (2005). Considering the above-cited elements could decrease C_{ant} inventories from Lo Monaco et al. (2005) in roughly 6–9 mol C m⁻² and get them closer to the rest of estimates.

If the $\Delta\Delta C_{\text{dis}}$ term here proposed was omitted (i.e., $\varphi=0$) then an average decrease of 6.8±2.8 mol C m⁻² in the specific inventory of C_{ant} would result (that is, 12% of the average C_{ant} inventory) (Fig. 6). This is in good agreement with the average 7% reduction factor proposed in Matsumoto and Gruber (2005). On the other hand, the long-term variation of A_T° produces an increase on the average specific inventory of 8.3±2.0 mol C m⁻². It must also be noticed that the influences of the $\Delta\Delta C_{\text{dis}}$ term and the long-term variation of A_T° in C_{ant} inventories vary little with latitude (Fig. 6).

The specific inventories for the Eastern and Western Atlantic basins are thoroughly detailed in Table 5 from Lee et al. (2003) for the same 10° latitude bands in this study. From that table, the inventories from the two Atlantic basins appear to be highly correlated ($\text{East}_{\text{inv.}}=1.069\text{West}_{\text{inv.}}-3.467$; $R^2=0.9246$). By calculating a west/east inventory ratio and applying it to our Eastern Atlantic results, we were able to come up with an estimate of the total inventory of C_{ant} for the Atlantic Ocean. In so doing, the uncertainties associated with the extrapolation due topographic effects would affect our results in the same manner as they would affect the ones in Lee et al. (2003). It must be noticed that the inventories between 50°–70° S and 60°–70° N estimated from our C_{ant} estimates are directly applied to calculate the total inventory. Knowingly of the caveats associated with the above practices, an estimate of 55±13 Pg C for the Atlantic C_{ant} total inventory was finally obtained for the φC_T° method. This result is substantially higher than recently calculated C_{ant} inventories (~18% larger) mainly due to the differences found in the Southern Ocean and Nordic Seas (Vázquez-Rodríguez et al., 2009).

Anthropogenic CO₂ in the Atlantic Ocean

M. Vázquez-Rodríguez
et al.

[Title Page](#)[Abstract](#)[Introduction](#)[Conclusions](#)[References](#)[Tables](#)[Figures](#)[◀](#)[▶](#)[◀](#)[▶](#)[Back](#)[Close](#)[Full Screen / Esc](#)[Printer-friendly Version](#)[Interactive Discussion](#)

5 Conclusions

The φC_T° method is a process-oriented geochemical approach that attempts to account for the nature and evolution of the phenomena that ultimately have affected the C_{ant} storage in the ocean since the 1750s. It considers from the biogeochemistry of the marine carbon cycle to the mixing and air-sea exchange processes that control the uptake of C_{ant} by the ocean. It also considers the spatiotemporal variability of the A_T° and ΔC_{dis} terms. The subsurface layer reference for WMF conditions has served to produce high-performance parameterizations of A_T° and ΔC_{dis} that can be used to estimate C_{ant} without the need of any additional and arbitrary zero- C_{ant} references. Overall, the proposed method upgrades translate into significant impacts on C_{ant} inventories and bring closer together the estimates obtained from classical C_T° -based methods and newly introduced C_{ant} calculation approaches like the TrOCA or the TTD (Vázquez-Rodríguez et al., 2009).

This modified method to calculate C_{ant} has the potential to be further improved by considering some of the following: a) incorporating a model of the spatial variability of the R_C stoichiometric ratio, which is presently assumed to be constant; b) applying a more robust and elaborate eOMP mixing analysis to convey the A_T° and ΔC_{dis} into the ocean interior. The OMP should include more end-members in accordance with the complexity of the circulation and mixing phenomena that occur in the Atlantic and, particularly, in the Southern Ocean; c) Refining the proposed $\Delta\Delta C_{\text{dis}}$ model.

Regarding $\Delta\Delta C_{\text{dis}}$, clear discrepancies between the estimates from this study and Matsumoto and Gruber (2005) have been described for the subtropical gyres. In addition, some studies (Lefèvre et al., 2004; Olsen et al., 2006) point towards a net decrease of the $\Delta f\text{CO}_2$ gradient in the subpolar gyres, which is likely caused by the recent changes of the Northern North Atlantic circulation patterns (Curry and Mauritzen, 2005). This $\Delta f\text{CO}_2$ trend would be opposite to one that can be expected from the WMLD approximation adopted in this work. Thence, a further refined function for $\Delta\Delta C_{\text{dis}}$ based on observations or synthetic data from OGCMs would be desirable. This

BGD

6, 4527–4571, 2009

Anthropogenic CO₂ in the Atlantic Ocean

M. Vázquez-Rodríguez
et al.

Title Page

Abstract

Introduction

Conclusions

References

Tables

Figures

◀

▶

◀

▶

Back

Close

Full Screen / Esc

Printer-friendly Version

Interactive Discussion



discrepancy between the detected decrease in the $p\text{CO}_2$ gradient and the supposed increase in ΔC_{dis} over time could stem from the separation between the natural and anthropogenic CO_2 signal. Unfortunately, these signals are impossible to discern using observational data and can only be estimated with the help of 3-D OGCMs. This is intended as prospective work.

Appendix A

The eOMP analysis is a method used to estimate the mixing proportions of a set of end-members that make up a particular water sample. It is desirable (but not compulsory) that the end-members are actually source water types (SWT) to grant some robustness to the eOMP. The use of eOMP is recommended (compared with the classical OMP) when the water mass analysis has a basin-wide breadth, or if the SWTs are to represent conditions in WMF regions remote from the region under investigation, meaning that biogeochemical changes can no longer be disregarded and have to be included in the analysis.

To resolve the mixing problem, the eOMP approach poses a set of linear equations built from conservative and non-conservative variables (Table 3) to conform an equation system that is solved by minimizing its residuals using a non-negative least square routine. In this study the tracers taken as conservative are θ , S and silicate whilst the non-conservative ones are oxygen, nitrate and phosphate. The conservative behaviour of silicate is assumed for eOMP resolution purposes given the high silicate values of the southern end-members compared to the northern ones (Table 3). Consciously of such north-south silicate gradient, assuming a conservative behaviour for silicate constitutes a plausible approximation because its biological perturbation would be negligible compared to the variability generated by the physical mixing.

Each equation in Table 3 was properly weighed according to the following criteria: tracers having the most accurate analytical determinations and/or lowest environmental variability were assigned the largest weights. By doing so, the residuals associated

BGD

6, 4527–4571, 2009

Anthropogenic CO_2 in the Atlantic Ocean

M. Vázquez-Rodríguez
et al.

Title Page

Abstract

Introduction

Conclusions

References

Tables

Figures

◀

▶

◀

▶

Back

Close

Full Screen / Esc

Printer-friendly Version

Interactive Discussion



to highly weighed equations are largely minimized (Poole and Tomczak, 1999). An inherent constraint to the system of equations is that the number of end-members that can be considered in an eOMP to resolve their mixing really depends on the number of variables available. Hence, given the set of seven (six plus the mass constraint) eOMP equations in Table 3, six end-members were defined in this work to resolve the mixing through the length of the Eastern Atlantic basin. They have been named as N1, N2, S1, S2, Weddell Sea Deep Water (WSDW) and Circumpolar Deep Water (CDW) (Figs. 2 and 7).

The mixing of northern water masses in the Eastern Atlantic basin has been simplified in this work by defining the N1 and N2 end-members (Figs. 2 and 7). Although none of them represents any known water source, they were characterized from the observed upper limits of the salinity and temperature variability ranges. Rigorously speaking, N1 is made up of about 13% of MW and 87% of LSW, which is one of the most important components of NADW. The N2 end-member has very similar thermohaline characteristics to the Denmark Strait Overflow Water (DSOW) that forms in the Greenland Sea (Strass et al., 1993). The Iceland-Scotland Overflow Water (ISOW: 1.9°C, 34.98) (Álvarez et al., 2004) can also be found along the mixing line established between N1 and N2.

On the Southern Ocean end, the linear mixing of different proportions of the S1 and S2 end-members can yield several water masses that form in the upper South Atlantic, namely: Antarctic Intermediate Water (AAIW), Sub-Antarctic Mode Water (SAMW), Ice Shelf Water (ISW) and Winter Water (WW) (Brea et al., 2004; Lo Monaco et al., 2005). Moreover, some deep-waters like the CDW and the Weddell Sea Deep Water (WSDW) are also found on this end of the Atlantic (Figs. 2 and 7). The CDW forms from the mixing of WSDW with deep waters from the three major oceans in the Antarctic Circumpolar Currents (Broecker et al., 1985; Onken, 1995; Brea et al., 2004). On the other hand, WSDW is formed from the mixing of ISW and the overlying Warm Deep Water in the Weddell Sea (Onken, 1995). The thermohaline type values of CDW listed in Table 3 were taken from measurements made at the Drake Passage (Broecker et

**Anthropogenic CO₂
in the Atlantic Ocean**M. Vázquez-Rodríguez
et al.

Title Page

Abstract

Introduction

Conclusions

References

Tables

Figures

◀

▶

◀

▶

Back

Close

Full Screen / Esc

Printer-friendly Version

Interactive Discussion



al., 1985). In the case of the type values for nitrate, phosphate and silicate for the six end-members in Fig. 7, they were obtained by extrapolation of the ad hoc properties from regression lines with S and θ (Poole and Tomczak, 1999). Afterwards, these preliminary type values were run through an iterative process as in Álvarez et al. (2004) in order to refine the estimates.

The A_T° and ΔC_{dis} type values in Table 3 were calculated by first identifying each end-member within the subsurface layer and then applying Eqs. (1) and (2), respectively. In the case of CDW, the former procedure to calculate A_T° and ΔC_{dis} cannot be applied. Even though the θ and S type values of this end-member are enclosed within the observed thermohaline subsurface variability (Figs. 2, 3a and b), the fact that this water mass forms off-bounds the Atlantic basin from the mixing of WSDW with deep waters from the three major oceans requires treating it separately. The θ - S type values for CDW here used (Table 3) were obtained from measurements at the Drake Passage (Broecker et al., 1985). To estimate the ΔC_{dis} and A_T° type values, the CDW was decomposed into its constituent proportions of North Atlantic Deep Water (NADW), Antarctic Intermediate Water (AAIW) and WSDW, after Broecker et al. (1985). According to Broecker et al. (1985) the CDW is formed by deep mixing of 25%, 45% and 30% of Northern component, Southern component and AAIW, respectively. The Southern component in Broecker et al. (1985) corresponds with the WDSW end-member in the present work, while the so-called Northern component is made up of 60% of N1 and 40% of the N2 end-members in this study. Finally, the AAIW in Broecker et al. (1985) would correspond to a mix of 93% of S1 and 7% of S2.

The obtained eOMP results show high correlation coefficients (R^2 , Table 3) and low standard errors of the residuals (Table 3) with the measured tracer concentrations. This means that the simplified mixing model here presented is able to reproduce with a high degree of confidence the physical and chemical variability observed in the Eastern Atlantic basin. In terms of reliability, the results here obtained are comparable to those in other studies, such as in Karstensen and Tomczak (1998) or Álvarez et al. (2004), for example.

Anthropogenic CO₂ in the Atlantic Ocean

M. Vázquez-Rodríguez
et al.

Title Page

Abstract

Introduction

Conclusions

References

Tables

Figures

◀

▶

◀

▶

Back

Close

Full Screen / Esc

Printer-friendly Version

Interactive Discussion



Acknowledgements. We would like to extend our gratitude to the Chief Scientists, scientists and the crew who participated and put their efforts in the oceanographic cruises utilized in this study, particularly to those responsible for the carbon, CFC, and nutrient measurements. This study was developed and funded by the European Commission within the 6th Framework Programme (EU FP6 CARBOOCEAN Integrated Project, Contract no. 511176), Ministerio de Educación y Ciencia (CTM2006-27116-E/MAR), Xunta de Galicia (PGIDIT05PXIC40203PM), Acción Integrada Hispano-Francesa (HF2006-0094) and the French research project OVIDE. M. Vázquez-Rodríguez is funded by Consejo Superior de Investigaciones Científicas (CSIC) I3P predoctoral grant program I3P-BPD2005. Funding for Richard G. J. Bellerby was provided from grant no. 511176 (GOCE).

References

- Álvarez, M., Pérez, F. F., Shoosmith, D. R., and Bryden H. L.: The unaccounted role of Mediterranean Water in the draw-down of anthropogenic carbon, *J. Geophys. Res.*, 110, 1–18, doi:10.1029/2004JC002633, 2005.
- Álvarez, M., Pérez, F. F., Bryden, H. L., and Ríos, A. F.: Physical and biogeochemical transports structure in the North Atlantic subpolar gyre, *J. Geophys. Res.*, 109, C03027, doi:10.1029/2003JC002015, 2004.
- Azetsu-Scott, K., Jones, E. P., Yashayaev, I., and Gershay, R. M.: Time series study of CFC concentrations in the Labrador Sea during deep and shallow convection regimes (1991–2000), *J. Geophys. Res.*, 108(C11), 3354, doi:10.1029/2002JC001317, 2003.
- Bates, N. R., Michaels, A. F., and Knap, A. H.: Seasonal and interannual variability of the oceanic carbon dioxide system at the U.S. JGOFS Bermuda Atlantic Time-series Site, *Deep-Sea Res. Pt. II*, 43(2–3), 347–383, 1996.
- Bellerby, R. G. J., Olsen, A., Furevik, T., and Anderson L. A.: Response of the surface ocean CO₂ system in the Nordic Seas and North Atlantic to climate change, in: *Climate Variability in the Nordic Seas*, edited by: Drange, H., Dokken, T. M., Furevik, T., Gerdes, R., and Berger, W., *Geophysical Monograph Series*, AGU, 189–198, 2005.
- Berelson, W. M., Balch, W. M., Najjar, R., Feely, R. A., Sabine, C., and Lee, K.: Relating estimates of CaCO₃ production, export, and dissolution in the water column to measurements of

BGD

6, 4527–4571, 2009

Anthropogenic CO₂ in the Atlantic Ocean

M. Vázquez-Rodríguez
et al.

Title Page

Abstract

Introduction

Conclusions

References

Tables

Figures

◀

▶

◀

▶

Back

Close

Full Screen / Esc

Printer-friendly Version

Interactive Discussion



**Anthropogenic CO₂
in the Atlantic Ocean**

M. Vázquez-Rodríguez
et al.

[Title Page](#)[Abstract](#)[Introduction](#)[Conclusions](#)[References](#)[Tables](#)[Figures](#)[◀](#)[▶](#)[◀](#)[▶](#)[Back](#)[Close](#)[Full Screen / Esc](#)[Printer-friendly Version](#)[Interactive Discussion](#)

CaCO₃ rain into sediment traps and dissolution on the sea floor: A revised global carbonate budget, *Global Biogeochem. Cy.*, 21, GB1024, doi:10.1029/2006GB002803, 2007.

5 Biastoch, A., Völker, C., and Böning, C. W.: Uptake and spreading of anthropogenic trace gases in an eddy-permitting model of the Atlantic Ocean, *J. Geophys. Res.*, 112, C09017, doi:10.1029/2006JC003966, 2007.

Brea S., Álvarez-Salgado, X. A., Álvarez, M., Pérez, F. F., Memery, L., Mercier, H., and Messias, M. J.: Nutrient mineralization rates and ratios in the Eastern South Atlantic, *J. Geophys. Res.*, 109, C05030, doi:10.1029/2003JC002051, 2004.

10 Brewer, P. G.: Direct observations of the oceanic CO₂ increase. *Geophys. Res. Lett.*, 5, 997–1000, 1978.

Brewer, P., Wong, G., Bacon, M., and Spencer, D.: An oceanic calcium problem? *Earth Planet. Sci. Lett.*, 26, 81–87, 1975.

Broecker, W. S.: “NO” a conservative water mass tracer, *Earth Planet. Sc. Lett.*, 23, 8761–8776, 1974.

15 Broecker, W. S. and Peng, T.-H.: *Tracers in the Sea*, Columbia University, Eldigio Press, New York, 690 pp., 1982.

Broecker, W. S., Takahashi, T., and Peng, T.-H.: Reconstruction of past atmospheric CO₂ contents from the chemistry of the contemporary ocean, Rep. DOE/OR-857, US Dept. of Energy, Washington, D. C., 79 pp., 1985.

20 Chen, C. T. and Millero, F. J.: Gradual increase of oceanic carbon dioxide, *Nature*, 277, 205–206, 1979.

Clayton, T. D. and Byrne, R. H.: Calibration of m-cresol purple on the total hydrogen ion concentration scale and its application to CO₂-system characteristics in seawater, *Deep Sea Res. Pt. I*, 40, 2115–2129, 1993.

25 Corbière A., Metzl, N., Reverdin, G., Brunet, C., and Takahashi, T.: Interannual and decadal variability of the oceanic carbon sink in the North Atlantic subpolar gyre, *Tellus*, 1–11, doi:10.1111/j.1600-0889.2006.00232.2007.

Curry, R., Dickson, B., and Yashahaev, I.: A change in the freshwater balance of the Atlantic Ocean over the past four decades, *Nature*, 426, 826–829, 2003.

30 Curry, R. and Mauritzen, C.: Dilution of the Northern North Atlantic in Recent Decades, *Science*, 308, 1772–1774, 2005.

Dickson, A. G. and Millero, F. J.: A comparison of the equilibrium constants for the dissociation of carbonic acid in seawater media, *Deep-Sea Res.*, 34A(10), 1733–1743, 1987.

DOE: Handbook of the Methods for the Analysis of the Various Parameters of the Carbon Dioxide System in Sea Water, Version 2, ORNL/CDIAC-74, edited by: Dickson, A. G. and Goyet, C., 1994.

Doney, S. C. and Jenkins, W. J.: The effect of boundary conditions on tracer estimates of thermocline ventilation rates, *J. Mar. Res.*, 46, 947–965, 1988.

Fine, R. A., Rhein, M., and Andrié, C.: Using a CFC effective age to estimate propagation and storage of climate anomalies in the deep western North Atlantic Ocean, *Geophys. Res. Lett.*, 29(24), 2227, doi:10.1029/2002GL015618, 2002.

Fraga, F. and Álvarez-Salgado, X. A.: On the variation of alkalinity during the photosynthesis of phytoplankton, *Cienc. Mar.*, 31, 627–639, 2005.

Friis, K.: A review of marine anthropogenic CO₂ definitions: introducing a thermodynamic approach based on observations, *Tellus*, 58B, 2–15, doi:10.1111/j.1600-0889.2005.00173.x, 2006.

Gruber, N.: Anthropogenic CO₂ in the Atlantic Ocean, *Global Biogeochem. Cy.*, 12, 165–191, 1998.

Gruber, N., Sarmiento, J. L., and Stocker, T. F.: An improved method for detecting anthropogenic CO₂ in the oceans. *Global Biogeochem. Cy.*, 10, 809–837, 1996.

Hall, T. M., Waugh, D. W., Haine, T. W. N., Robbins, P. E., and Khatiwala, S.: Estimates of anthropogenic carbon in the Indian Ocean with allowance for mixing and time-varying air-sea CO₂ disequilibrium, *Global Biogeochem. Cy.*, 18, GB1031, doi:10.1029/2003GB002120, 2004.

Harvey, H. W.: *The Chemistry and Fertility of Sea Waters*, 2nd edn., Cambridge Univ. Press, New Cork, 240 pp., 1969.

Heinze, C.: Simulating oceanic CaCO₃ export production in the greenhouse, *Geophys. Res. Lett.*, 31, L16308, doi:10.1029/2004GL020613, 2004.

Honjo, S. and Manganini, S. J.: Annual biogenic particle fluxes to the interior of the North Atlantic Ocean; studied at 34° N 21° W, *Deep-Sea Res.*, 40, 587–607, 1993.

IPCC: Summary for Policymakers, in: *Climate Change 2007: Impacts, Adaptation and Vulnerability. Contribution of Working Group II to the Fourth Assessment Report of the Intergovernmental Panel on Climate Change*, Cambridge University Press, Cambridge, UK, 7-22, 2007.

Karstensen, J. and Tomczak, M.: Age determination of mixed water masses using CFC and oxygen data, *J. Geophys. Res. Oceans*, 103(C9), 18599–18609, 1998.

BGD

6, 4527–4571, 2009

Anthropogenic CO₂ in the Atlantic Ocean

M. Vázquez-Rodríguez
et al.

Title Page

Abstract

Introduction

Conclusions

References

Tables

Figures

◀

▶

◀

▶

Back

Close

Full Screen / Esc

Printer-friendly Version

Interactive Discussion



- Körtzinger, A., Mintrop, L., and Duinker, J. C.: On the penetration of anthropogenic CO₂ into the North Atlantic ocean, *J. Geophys. Res.*, 103, 18681–18689, 1998.
- Lab Sea Group: The Labrador Sea Deep Convection Experiment, *B. Am. Meteorol. Soc.*, 79(10), 2033–2058, 1998.
- 5 Lefèvre, N., Watson, A. J., Olsen, A., Ríos, A. F., Pérez, F. F., and Johannessen, T.: A decrease in the sink for atmospheric CO₂ in the North Atlantic, *Geophys. Res. Lett.*, 31, L07306, doi:10.1029/2003GL018957, 2004.
- Lee, K., Choi, S.-D., Park, G.-H., Wanninkhof, R., Peng, T.-H., Key, R. M., Sabine, C. L., Feely, R. A., Bullister, J. L., Millero, F. J., and Kozyr, A.: An updated anthropogenic CO₂ inventory in the Atlantic Ocean, *Global Biogeochem. Cy.*, 17(4), 1116, doi:10.1029/2003GB002067, 2003.
- 10 Levitus, S. et al.: Anthropogenic warming of the earth's climate system, *Science*, 292, 267–270, 2001.
- Lo Monaco, C., Metzl, N., Poisson, A., Brunet, C., and Schauer, B.: Anthropogenic CO₂ in the SO: Distribution and inventory at the Indian-Atlantic boundary (World Ocean Circulation Experiment line I6), *J. Geophys. Res.*, 110, C06010, doi:10.1029/2004JC002643, 2005.
- 15 Lüger, H., Wallace, D. W. R., Körtzinger, A., and Nojiri, Y.: The pCO₂ variability in the midlatitude North Atlantic Ocean during a full annual cycle, *Global Biogeochem. Cy.*, 18, GB3023, doi:10.1029/2003GB002200, 2004.
- 20 Martin, J. H., Fitzwater, S. E., Gordon, R. M., Hunter, C. N., and Tanner, S. J.: Iron, primary production and carbon-nitrogen flux studies during the JGOFS North Atlantic Bloom Experiment, *Deep-Sea Res. Pt. II*, 40, 641–653, 1993.
- Matear, R. J., Wong, C. S., and Xie, L.: Can CFCs be used to determine anthropogenic CO₂? *Global Biogeochem. Cy.*, 17(1), 1013, doi:10.1029/2001GB001415, 2003.
- 25 Matsumoto, K. and Gruber, N.: How accurate is the estimation of anthropogenic carbon in the ocean? An evaluation of the ΔC* method, *Global Biogeochem. Cy.*, 19, GB3014, doi:10.1029/2004GB002397, 2005.
- Millero, F. J., Zhang, J. Z., Lee, K., and Campbell, D. M.: Titration alkalinity of seawater, *Mar. Chem.*, 44, 153–156, 1993.
- 30 Millero, F. J., Lee, K., and Roche, M.: Distribution of alkalinity in the surface waters of the major oceans, *Mar. Chem.*, 60, 95–110, 1998.
- Milliman, J. D., Troy, P. J., Bakch, W. M., Adams, A. K., Li, Y.-H., and Mackenzie, F. T.: Biologically mediated dissolution of calcium carbonate above the chemical lysocline? *Deep-Sea*

Anthropogenic CO₂ in the Atlantic Ocean

M. Vázquez-Rodríguez
et al.

[Title Page](#)[Abstract](#)[Introduction](#)[Conclusions](#)[References](#)[Tables](#)[Figures](#)[◀](#)[▶](#)[◀](#)[▶](#)[Back](#)[Close](#)[Full Screen / Esc](#)[Printer-friendly Version](#)[Interactive Discussion](#)

Res. Pt. I, 46, 1653–1669, 1999.

Mintrop, L., Perez, F. F., Gonzalez-Davila, M., Santana-Casiano, M. J., and Kortzinger, A.: Alkalinity determination by potentiometry: Intercalibration using three different methods, *Cienc. Mar.*, 26(1), 23–37, 2002.

5 Naegler, T., Ciais, P., Rodgers, K., and Levin, I.: Excess radiocarbon constraints on air-sea gas exchange and the uptake of CO₂ by the oceans, *Geophys. Res. Lett.*, 33, L11802, doi:10.1029/2005GL025408, 2006.

Olsen, A., Omar, A. M., and Bellerby, R. G. J.: Magnitude and origin of the anthropogenic CO₂ increase and 13C Suess effect in the Nordic seas since 1981, *Global Biogeochem. Cy.*, 20, GB3027, doi:10.1029/2005GB002669, 2006.

10 Onken, R.: The spreading of Lower Circumpolar Deep Water into the Atlantic Ocean, *J. Phys. Oceanogr.*, 25, 3051–3063, 1995.

Ono, T., Watanabe, S., Okuda, K., and Fukasawa, M.: Distribution of total carbonate and related properties in the North Pacific along 30E N, *J. Geophys. Res.*, 103, 30873–30883, 1998.

15 Orsi, A. H., Smethie Jr., W. M., and Bullister, J. L.: On the total input of Antarctic waters to the deep ocean: A preliminary estimate from chlorofluorocarbon measurements, *J. Geophys. Res.*, 107(C8), 3122, doi:10.1029/2001JC000976, 2002.

Pérez, F. F., Mouriño, C., Fraga, F., and Ríos, A. F.: Displacement of water masses and remineralization rates off the Iberian Peninsula by nutrient anomalies. *J. Mar. Res.*, 51(4), 869–892, 1993.

20 Pérez, F. F. and Fraga, F.: A precise and rapid analytical procedure for alkalinity determination. *Mar. Chem.*, 21, 169–182, 1987.

Pérez, F. F., Álvarez, M., and Ríos, A. F.: Improvements on the back-calculation technique for estimating anthropogenic CO₂, *Deep-Sea Res. Pt. I*, 49, 859–875, 2002.

25 Poole, R. and Tomczak, M.: Optimum multiparameter analysis of the water mass structure in the Atlantic Ocean thermocline, *Deep Sea Res. Pt. I*, 46, 1895–1921, 1999.

Pond, S. and Pickard, G. L.: *Introductory Dynamical Oceanography*, 2nd edn, Pergamon Press, Massachusetts, USA, 329 pp., 1983.

Rhein, M. and Hinrichsen, H. H.: Modification of Mediterranean water in the Gulf of Cadiz, studied with hydrographic, nutrient and chlorofluoromethane data, *Deep-Sea Res. Pt. I*, 40(2), 267–291, 1993.

30 Riebesell, U., Zondervan, I., Rost, B., Tortell, P. D., Zeebe, R. E., and Morel, F. M. M.: Reduced calcification of marine plankton in response to increased atmospheric CO₂, *Nature*, 407,

BGD

6, 4527–4571, 2009

Anthropogenic CO₂ in the Atlantic Ocean

M. Vázquez-Rodríguez
et al.

Title Page

Abstract

Introduction

Conclusions

References

Tables

Figures

◀

▶

◀

▶

Back

Close

Full Screen / Esc

Printer-friendly Version

Interactive Discussion



364–367, 2000.

Ríos, A. F., Álvarez-Salgado, X. A., Pérez, F. F., Bingler, L. S., Arístegui, J., and Mémerly, L.: Carbon dioxide along WOCE line A14: water masses characterization and anthropogenic entry, *J. Geophys. Res.*, 108(C4), 3123, doi:10.1029/2000JC000366, 2003.

5 Ríos, A. F., Johnson, K. M., Álvarez-Salgado, X. A., Arlen, L., Billant, A., Bingler, L. S., Branellec, P., Castro, C. G., Chipman, D. W., Rosón, G., and Wallace, D. W. R.: Carbon dioxide, hydrographic, and chemical data obtained during The R/V Maurice Ewing Cruise in the South Atlantic Ocean (WOCE Section A17, 4 January–21 March 1994), Carbon Dioxide Information Analysis Center, Oak Ridge National Laboratory, ORNL/CDIAC-148, NDP-084, 1–27, 10 Oak Ridge, Tennessee, USA, 2005.

Ríos, A. F., Anderson, T. R., and Pérez, F. F.: The carbonic system distribution and fluxes in the NE Atlantic during Spring 1991, *Prog. Oceanog.*, 35, 295–314, 1995.

Rosenheim, B. E., Swart, P. K., Thorrold, S. R., Eisenhauer, A., and Willenz, P.: Salinity change in the subtropical Atlantic: Secular increase and teleconnections to the North Atlantic Oscillation, *Geophys. Res. Lett.*, 32, L02603, doi:10.1029/2004GL021499, 2005.

15 Royal Society: Ocean acidification due to increasing atmospheric carbon dioxide, Document 12/05, Royal Society, London, ISBN-0-85403-617-2, 68 pp., 2005.

Sabine C. L., Feely, R. A., Gruber, N., Key, R. M., Lee, K., Bullister, J. L., Wanninkhof, R., Wong, C. S., Wallace, D. W. R., Tilbrook, B., Millero, F. J., Peng, T.-H., Kozyr, A., Ono, T., 20 and Ríos, A. F.: The oceanic sink for anthropogenic CO₂, *Science*, 305, 367–371, 2004.

Sabine, C. L. and Feely, R. A.: Comparison of recent Indian Ocean anthropogenic CO₂ estimates with a historical approach, *Global Biogeochem. Cy.*, 15(1), 31–42, 2001.

Sabine, C. L., Key, R. M., Johnson, K. M., Millero, F. J., Poisson, A., Sarmiento, J. L., Wallace, D. W. R., and Winn, C. D.: Anthropogenic CO₂ inventory of the Indian Ocean, *Global Biogeochem. Cy.*, 13, 179–198, 1999.

Santana-Casiano, J. M., Gonzalez-Davila, M., and Laglera, L. M.: The carbon dioxide system in the Strait of Gibraltar, *Deep-Sea Res. Pt. II*, 49, 4145–4161, 2002.

25 Sarma, V. V. S. S., Ono, T., and Saino, T.: Increase of total alkalinity due to shoaling of aragonite saturation horizon in the Pacific and Indian Oceans: Influence of anthropogenic carbon inputs, *Geophys. Res. Lett.*, 29(20), 1971, doi:10.1029/2002GL015135, 2002.

Siegenthaler, U. and Sarmiento, J.: Atmospheric carbon dioxide and the ocean, *Nature*, 365, 119–125, 1993.

Strass, V. H., Fahrbach, E., Schauer, U., and Sellmann, L.: Formation of Denmark Strait Over-

BGD

6, 4527–4571, 2009

Anthropogenic CO₂ in the Atlantic Ocean

M. Vázquez-Rodríguez
et al.

Title Page

Abstract

Introduction

Conclusions

References

Tables

Figures

◀

▶

◀

▶

Back

Close

Full Screen / Esc

Printer-friendly Version

Interactive Discussion



flow Water by mixing in the East Greenland Current, *J. Geophys. Res.*, 98, 6907–6919, 1993.

Takahashi, T., Sutherland, S. C., Sweeney, C., Poisson, A., Metz, N., Tilbrook, B., Bates, N., Wanninkhof, R., Feely, R. A., Sabine, C., Olafsson, J., and Nojiri, Y., Global sea-air CO₂ flux based on climatological surface ocean pCO₂, and seasonal biological and temperature effects, *Deep Sea Res. Pt. II*, 49, 1601–1622, 2002.

Thomas, H. and Ittekkot, V.: Determination of anthropogenic CO₂ in the North Atlantic Ocean using water mass ages and CO₂ equilibrium chemistry, *J. Mar. Sys.*, 27, 325–336, 2001.

Touratier, F., Azouzi, L., and Goyet, C.: CFC-11, Δ14C and ³H tracers as a means to assess anthropogenic CO₂ concentrations in the ocean, *Tellus*, 59B, 318–325, doi:10.1111/j.1600-0889.2006.00247.x, 2007.

Vázquez-Rodríguez, M., Touratier, F., Lo Monaco, C., Waugh, D. W., Padin, X. A., Bellerby, R. G. J., Goyet, C., Metz, N., Ríos, A. F., and Pérez, F. F.: Anthropogenic carbon distributions in the Atlantic Ocean: data-based estimates from the Arctic to the Antarctic, *Biogeosciences*, 6, 439–451, 2009, <http://www.biogeosciences.net/6/439/2009/>.

Wallace, D. W. R.: Storage and transport of Excess CO₂ in the Oceans: The JGOFS/WOCE Global CO₂ Survey: Ocean Circulation and Climate, edited by: Siedler, G., Church, J., and Gould, J., 489–521, Academic Press, San Diego – California, 2001.

Wanninkhof, R., Peng, T. H., Huss, B., Sabine, C. L., and Lee, K.: Comparison of inorganic carbon system parameters measured in the Atlantic Ocean from 1990 to 1998 and recommended adjustments, ORNL/CDIAC-140, Oak Ridge Natl. Lab., US Dept. of Energy, Oak Ridge, Tenn, 43 pp., 2003.

Wanninkhof, R., Doney, S. C., Peng, T. H., Bullister, J. L., Lee, K., and Feely, R. A.: Comparison of methods to determine the anthropogenic CO₂ invasion into the Atlantic Ocean. *Tellus*, 51B, 511–530, 1999.

Waugh, D. W., Hall, T. M., McNeil, B. I., Key, R., and Matear, R. J.: Anthropogenic CO₂ in the oceans estimated using transit time distributions, *Tellus B*, 58B, 376–389, doi:10.1111/j.1600-0889.2006.00222.x, 2006.

BGD

6, 4527–4571, 2009

Anthropogenic CO₂ in the Atlantic Ocean

M. Vázquez-Rodríguez
et al.

Title Page

Abstract

Introduction

Conclusions

References

Tables

Figures

◀

▶

◀

▶

Back

Close

Full Screen / Esc

Printer-friendly Version

Interactive Discussion



Anthropogenic CO₂
in the Atlantic Ocean

M. Vázquez-Rodríguez
et al.

Table 1. List of selected Atlantic cruises (Fig. 1). Only data collected at depths greater than 100 m was used for calculations. Surface layer data was discarded to avoid the influence of seasonal variability on C_{ant} estimates.

Section	Date	P.I.	Parameters Analyzed										Adjustments		
			C _T	A _T	fCO ₂	pH	Freons	N	P	Si	O	C _T	A _T		
A02	6 Nov–7 Mar 1997	P. Koltermann	Y ^a	Y	N ^b	N	Y	Y	Y	Y	Y	Y	Y	NA ^c	NA
AR01	23 Jan–24 Feb 1998	K. Lee	Y	Y	Y	Y	Y	Y	Y	Y	Y	Y	Y	NA	NA
A14	1 Nov–2 Nov 1995	H. Mercier	Y	Y+Calc ^d	N	N	Y	Y	Y	Y	Y	Y	Y	NA	NA
A16	4 Jul–29 Aug 1993	R. Wanninkhof	Y	Y	Y	Y	Y	Y	Y	Y	Y	Y	Y	NA	NA
A16N	4 Jun–11 Aug 2003	J. Bullister	Y	Y	Y	Y	Y	Y	Y	Y	Y	Y	Y	NA	NA
A17	1 Apr–21 Mar 1994	L. Memery	Y	Y+Calc	N	Y	Y	Y	Y	Y	Y	Y	Y	NA	–8 ^e
A20	17 Jul–10 Aug 1997	R. Pickart	Y	Y	Y	N	Y	Y	Y	Y	Y	Y	Y	NA	NA
A25 (OVIDE)	6 Jun–5 Jul 2002	H. Mercier	N	Y	Y	Y	Y	Y	Y	Y	Y	Y	Y	NA	NA
I06-Sa	23 Jan–9 Mar 1993	A. Poisson	Y	Y	Y	N	Y	Y	Y	Y	Y	Y	Y	NA	NA
I06-Sb	20 Feb–22 Mar 1996	A. Poisson	Y	Y	Y	N	Y	Y	Y	Y	Y	Y	Y	NA	NA
NSeas	1 Jun–7 Jun 2002	R. Bellerby	Y	Y	N	N	Y	Y	Y	Y	Y	Y	Y	NA	NA

Acronyms and superscripts denote the following:

^a Y=measured values available;

^b N=measured values unavailable;

^c NA=no adjustment made;

^d Y+Calc=When direct measurements were unavailable, A_T was calculated from C_T and pH measurements, using the thermodynamic relationships of the carbon system;

^e =Correction in μmol kg⁻¹, after ORNL/CDIAC 148 report

Title Page

Abstract

Introduction

Conclusions

References

Tables

Figures

◀

▶

◀

▶

Back

Close

Full Screen / Esc

Printer-friendly Version

Interactive Discussion



Anthropogenic CO₂ in the Atlantic Ocean

M. Vázquez-Rodríguez
et al.

Table 2. Coefficients and statistics for the Multilinear Regression (MLR) of ΔC_{dis} vs. conservative parameters (Eq. 3). Except for θ (°C) and S, all other variables and standard errors are given in $\mu\text{mol kg}^{-1}$. N stands for the number of valid points used for the fit, and R^2 is the correlation coefficient of the adjustment. The standard error of the estimate was calculated as σ/\sqrt{N} .

Region	Latitude Band	θ Interval [°C]	a	b ($\theta-10$)	c (S-35)	d (NO-300)	e (PO-300)	N	R^2	Std. error
Atlantic	[70° S–70° N]	$5 \leq \theta < 8$	-7.1 ± 1.0	1.29 ± 0.32	11.1 ± 1.0	*	*	138	0.62	4.1
N. Atl.	(20° N–70° N)	$8 \leq \theta < 18$	-13.4 ± 1.5	1.18 ± 0.46	*	*	0.17 ± 0.03	454	0.40	5.7
N. Atl.	(20° N–70° N)	$18 \leq \theta \leq 25$	-38.6 ± 3.0	1.67 ± 0.39	16.3 ± 1.4	-0.32 ± 0.07	0.52 ± 0.05	272	0.55	6.7
Intertrop.	[20° S–20° N]	$8 \leq \theta < 18$	-14.4 ± 0.6	2.39 ± 0.13	*	*	*	441	0.43	5.0
Intertrop.	[20° S–20° N]	$18 \leq \theta \leq 25$	-3.9 ± 3.5	2.55 ± 0.48	11.3 ± 2.4	*	*	125	0.18	7.1
S. Atl.	[70° S–20° S)	$8 \leq \theta < 18$	-10.7 ± 2.6	-1.82 ± 0.65	9.7 ± 2.4	-0.12 ± 0.04	-0.13 ± 0.04	232	0.31	4.0
S. Atl.	(70° S–20° S)	$18 \leq \theta \leq 25$	-38.6 ± 3.0	1.67 ± 0.39	16.3 ± 1.4	-0.32 ± 0.07	0.52 ± 0.05	272	0.55	6.7

Title Page

Abstract

Introduction

Conclusions

References

Tables

Figures

⏪

⏩

◀

▶

Back

Close

Full Screen / Esc

Printer-friendly Version

Interactive Discussion



**Anthropogenic CO₂
in the Atlantic Ocean**

M. Vázquez-Rodríguez
et al.

Table 3. The equations, weights and type values of the selected end-members for the eOMP. The correlation coefficient (R^2) between eOMP results and observed properties and the standard errors of these estimates are also listed. All type values and standard errors are given in $\mu\text{mol kg}^{-1}$ except for θ ($^{\circ}\text{C}$) and S. Notice that neither the A_T° nor the ΔC_{dis} equations (dark grey shade) belong to the system of equations for the eOMP (no weight assigned). The type values here listed were calculated a posteriori and are given as reference for the end-members here chosen.

Property	Equation	N1	N2	S1	S2	CDW	WSDW	Weight	R^2	Std. err.
θ	$\theta = \sum \theta_i^{\circ} X_j$	5	-1.1	5	-1.7	1.5	-0.7	8	0.9998	0.021
S	$S = \sum S_i^{\circ} X_j$	35.20	34.88	33.90	34.00	34.70	34.65	3	0.997	0.011
Si	$S_i = \sum S_{ij}^{\circ} X_j$	11	6	16	72	106	160	2	0.996	2.8
O ₂	$O_2 = \sum O_{2i}^{\circ} X_j - \text{AOU}$	307	358	309	366	336	355	1.6	0.995	3.5
NO ₃	$\text{NO}_3 = \sum \text{NO}_{3i}^{\circ} X_j + \text{AOU}/R_N$	10.5	9.8	20.6	37.0	15.1	20.5	1.7	0.996	0.5
PO ₄	$\text{PO}_4 = \sum \text{PO}_{4i}^{\circ} X_j + \text{AOU}/R_P$	0.63	0.67	1.43	2.60	1.07	1.48	1.5	0.993	0.04
Mass	$1 = \sum X_j$	*	*	*	*	*	*	100	*	*
A_T°	$A_T^{\circ} = \sum A_{Ti}^{\circ} X_j$	2310	2286	2282	2344	2319	2347	*	*	*
ΔC_{dis}	$\Delta C_{\text{dis}}^{\circ} = \sum \Delta C_{\text{dis}i}^{\circ} X_j$	-7	-21	0	-5	-23	-30	*	*	*

Title Page

Abstract

Introduction

Conclusions

References

Tables

Figures

◀

▶

◀

▶

Back

Close

Full Screen / Esc

Printer-friendly Version

Interactive Discussion



Anthropogenic CO₂ in the Atlantic Ocean

M. Vázquez-Rodríguez
et al.

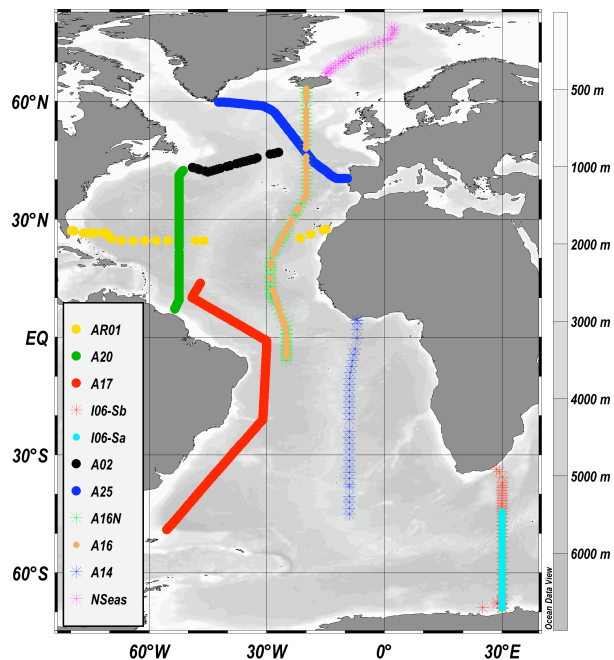


Fig. 1. Map showing Atlantic cruises used to characterise the subsurface layer. The cruises denoted by stars were also selected for testing the adequacy of proposed modifications in C_{ant} estimation (Sect. 4).

Title Page

Abstract

Introduction

Conclusions

References

Tables

Figures

◀

▶

◀

▶

Back

Close

Full Screen / Esc

Printer-friendly Version

Interactive Discussion



Anthropogenic CO₂
in the Atlantic Ocean

M. Vázquez-Rodríguez
et al.

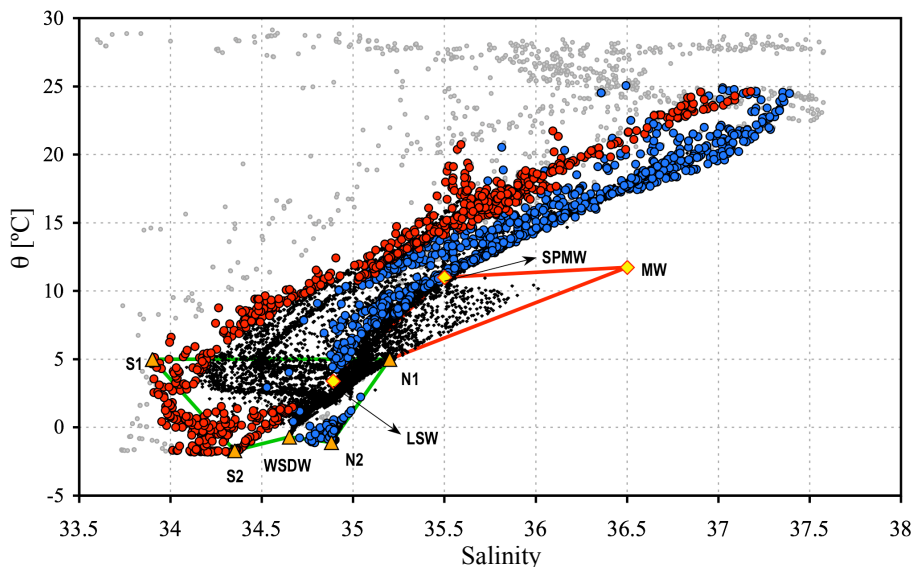


Fig. 2. TS diagram of the Atlantic from the studied dataset (Fig. 1 and Table 1). Red circles represent South Atlantic subsurface (100–200 m) waters and blue circles are North Atlantic subsurface waters. The smaller dark dots represent samples collected deeper than 200 m. The small light-grey dots are the uppermost 25 m surface waters, showing a clear distinction from the rest of the tightly-wrapped bulk of samples. The thick yellow diamonds joined with the red line are the end-members that define the mixing triangle used to resolve the influence of Mediterranean Water (Sect. 3). The thick orange triangles joined by the green line are the end-members used in the extended Optimum Multiparameter (eOMP) mixing analysis used to calculate A_T^o and ΔC_{dis} in waters below the 5°C isotherm (Sect. 3).

Title Page

Abstract

Introduction

Conclusions

References

Tables

Figures

◀

▶

◀

▶

Back

Close

Full Screen / Esc

Printer-friendly Version

Interactive Discussion



Anthropogenic CO₂
in the Atlantic Ocean

M. Vázquez-Rodríguez
et al.

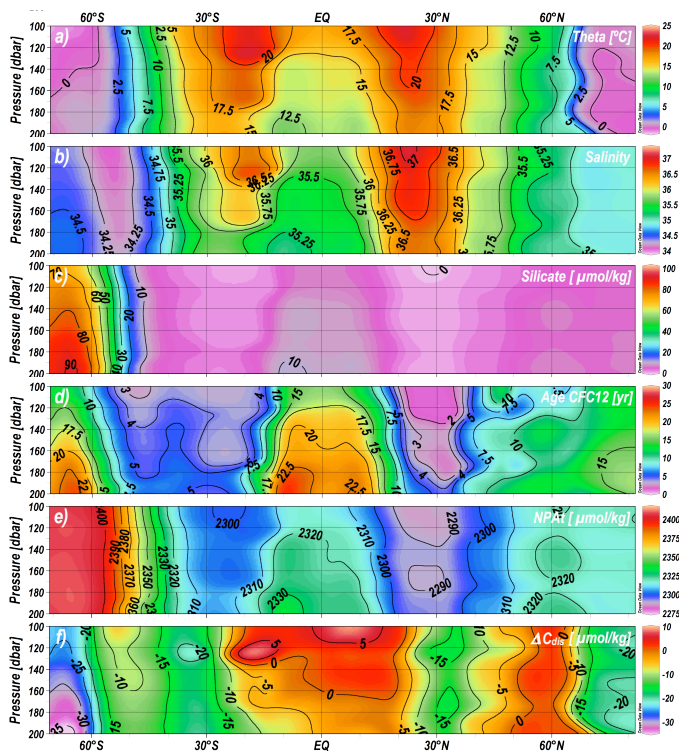


Fig. 3. Subsurface layer (100–200 m) distributions of several properties from the selected Atlantic cruises (Fig. 1): **(a)** Potential temperature (θ , in $^{\circ}\text{C}$); **(b)** Salinity; **(c)** Silicate ($\mu\text{mol kg}^{-1}$); **(d)** Age estimates from CFC12 data (years); **(e)** NPA_T ($\mu\text{mol kg}^{-1}$); **(f)** ΔC_{dis} ($\mu\text{mol kg}^{-1}$) calculated from the original definition in Gruber et al. (1996) (see Eq. 2).

Title Page

Abstract

Introduction

Conclusions

References

Tables

Figures



Back

Close

Full Screen / Esc

Printer-friendly Version

Interactive Discussion



Anthropogenic CO₂ in the Atlantic Ocean

M. Vázquez-Rodríguez
et al.

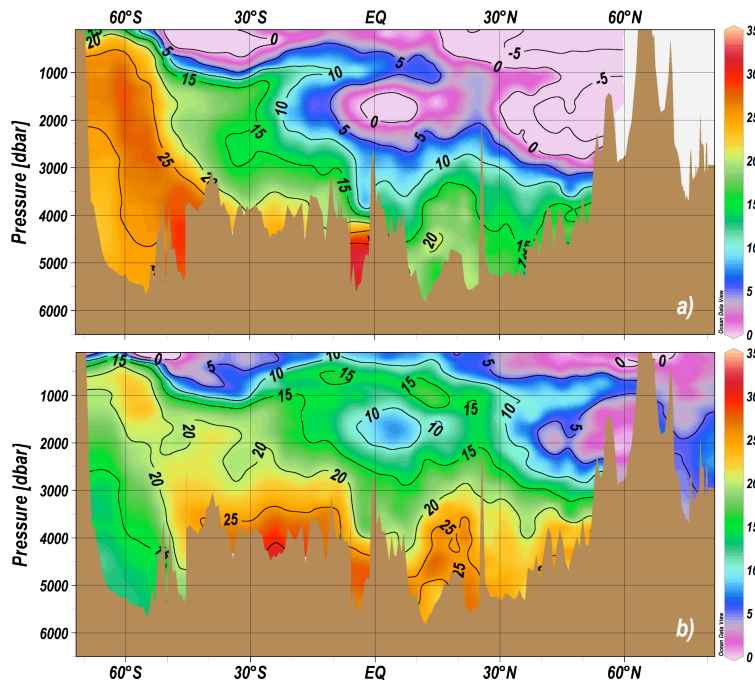


Fig. 4. Distributions of computed CaCO₃ dissolution (ΔCa , in $\mu\text{mol kg}^{-1}$) using: **(a)** the A_T° parameterization from Lee et al. (2003). The light-purple blur indicates negative ΔCa estimates (CaCO₃ precipitation). Only the isopleth of $-5 \mu\text{mol kg}^{-1}$ was added in this region as a reference, but values of ΔCa as low as $-17 \mu\text{mol kg}^{-1}$ are reached; **(b)** the A_T° parameterization in Eq. (1) from this study.

Title Page

Abstract

Introduction

Conclusions

References

Tables

Figures

◀

▶

◀

▶

Back

Close

Full Screen / Esc

Printer-friendly Version

Interactive Discussion



Anthropogenic CO₂
in the Atlantic Ocean

M. Vázquez-Rodríguez
et al.

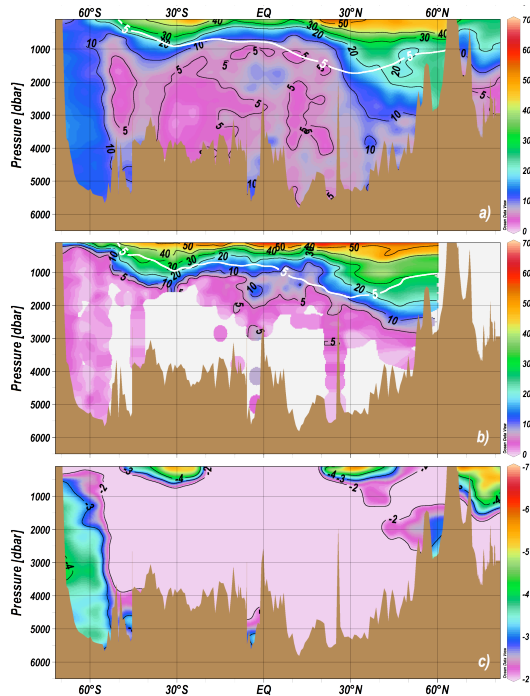


Fig. 5. C_{ant} distributions ($\mu\text{mol kg}^{-1}$) of the Eastern Atlantic basin calculated with: **(a)** The φC_T^C method and **(b)** The ΔC^* method as of Lee et al. (2003) for latitudes below 60°N , where their A_T^C parameterization is valid. Negative C_{ant} estimates are omitted and shown as blank areas. The thick white isoline in **(a)** and **(b)** is the 5°C isotherm to indicate the regions where A_T^C and ΔC_{dis} are calculated with different procedures, according to the φC_T^C method. The effect of the “ φ ” term in individual C_{ant} estimates is shown in **(c)** (in $\mu\text{mol kg}^{-1}$). This was calculated by subtracting C_{ant} calculated from Eq. (10) with $\varphi=0$ and then $\varphi=0.55$. The results have been referenced to 1994.

Title Page

Abstract

Introduction

Conclusions

References

Tables

Figures

◀

▶

◀

▶

Back

Close

Full Screen / Esc

Printer-friendly Version

Interactive Discussion



Anthropogenic CO₂ in the Atlantic Ocean

M. Vázquez-Rodríguez
et al.

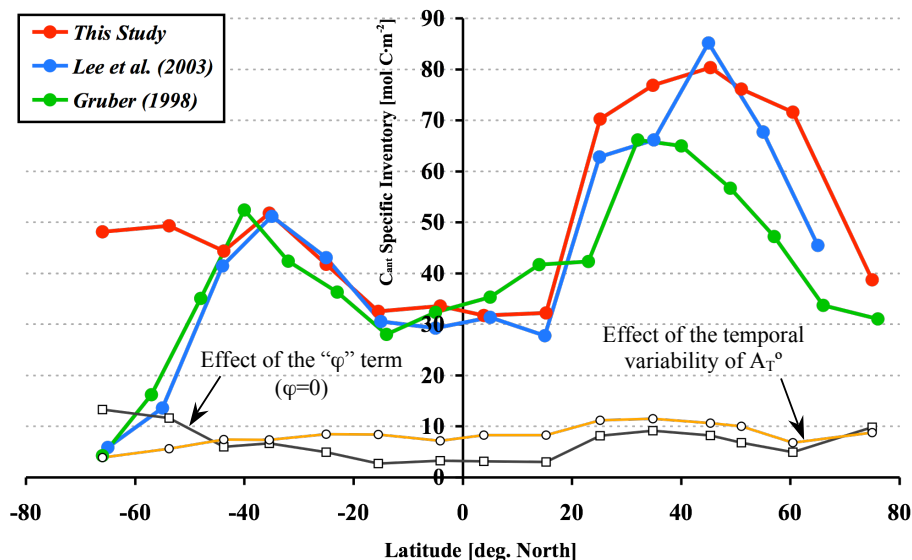


Fig. 6. Comparison of specific inventories of C_{ant} (mol C m^{-2}) of the Eastern Atlantic calculated using the ΔC^* method as in Gruber et al. (1996) (green line), the ΔC^* method as in Lee et al. (2003) (blue line) and the φC_T^0 method (red line). All inventory results were averaged by latitude bands and referenced to 1994, after Lee et al. (2003). The orange line with open circles gives the magnitude of the combined effects on the inventories of CaCO_3 and increasing SST, introduced through the PA_T^0 parameterization given in Eq. (1). The grey line with open squares represents the individual contribution to the φC_T^0 specific inventory of the φ term (i.e., when $\varphi=0$).

Title Page

Abstract

Introduction

Conclusions

References

Tables

Figures

◀

▶

◀

▶

Back

Close

Full Screen / Esc

Printer-friendly Version

Interactive Discussion



Anthropogenic CO₂ in the Atlantic Ocean

M. Vázquez-Rodríguez
et al.

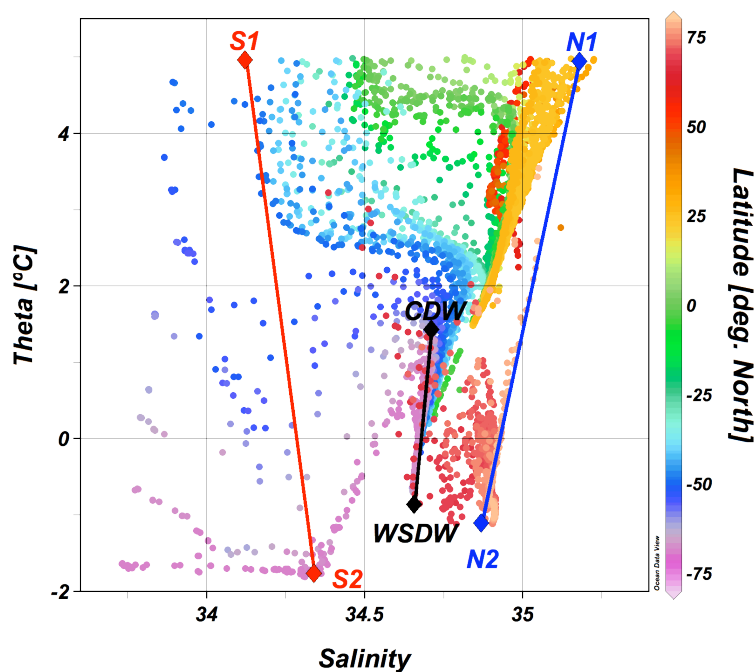


Fig. 7. A detailed view of the cold end ($\theta < 5^{\circ}\text{C}$) of the TS diagram in Fig. 2 showing the end-members defined to resolve the eOMP and the mixing lines between North Atlantic, South Atlantic and Southern Ocean waters. In order to differentiate Arctic waters from Antarctic waters in the mixing problem the samples were colour-graded according to their latitude of precedence.

Title Page

Abstract

Introduction

Conclusions

References

Tables

Figures

◀

▶

◀

▶

Back

Close

Full Screen / Esc

Printer-friendly Version

Interactive Discussion

